SOUTHAMPTON OCEANOGRAPHY CENTRE

SOC Internal Document No. 46

Evaluation of the Acoustic Correlation Current Profiler on *Discovery* cruise 223

S. Bacon and E. C. Kent

1999

James Rennell Division
Southampton Oceanography Centre
Empress Dock
Southampton SO14 3ZH, U. K.
Tel: +44 1703 596441
Fax: +44 1703 596204
Email: S.Bacon@soc.soton.ac.uk

Document Data Sheet:

Authors: Sheldon Bacon and Elizabeth C. Kent

Publication Date: 1999

Title: Evaluation of the Acoustic Correlation Current Profiler on *Discovery* cruise 223.

Reference: Southampton Oceanography Centre Internal Document, No. 46, 48 pp.

Abstract: We present acoustic correlation current profiler (ACCP) data collected during *Discovery* cruise 223 and analyse its performance, in terms of %good, depth penetration, standard deviation of velocity per time / depth bin, as a function of various other parameters: wind speed, significant wave height, relative wind direction and ship speed. We compare ACCP currents with currents measured at the same time by acoustic Doppler current profilers (ADCPs), both vessel-mounted (VM-ADCP) and lowered (L-ADCP). Mainly the results are disappointing: the ACCP routinely profiles down only to about 600 m; there is near-zero data return in poor weather (moderate to high winds and waves); even deep profiles, down to *ca.* 1500 m on station in calm weather show much scatter and some divergence from L-ADCP profiles.

Keywords: North Atlantic; *Discovery* cruise 223; Acoustic Correlation Current Profiler, ACCP.

Issuing Organisation:

Southampton Oceangraphy Centre, Empress Dock, Southampton SO14 3ZH, U. K. Tel 01703 596116. Director Prof. John Shepherd.

Not generally distributed – please refer to authors.

CONTENTS

LIST OF TABLES

LIST OF FIGURES

1. INTRODUCTION

In this report, we evaluate the performance of an RDI 22 kHz acoustic correlation current profiler (ACCP) carried on RRS *Discovery* during cruise 223 in late 1996 (Leach and Pollard, 1998: the cruise report). We will not rehearse here the operating principles of the ACCP, which are described elsewhere: see Griffiths, Bradley and Murdock (1999; GBM hereafter) for a current list of references.

The cruise was notable for its rather foul weather. This impinged severely on the performance of the ACCP. Days would pass without a good measurement being made. Accordingly, it was deemed a waste of time to record continuously from the ACCP; instead, periods of moderate weather were awaited before beginning recording. Thus we acquired data over four separate periods totalling about 9 days. The cruise track is shown in figure 1.1, on which is also shown the four recording periods, numbered 2 to 5. For later reference we also show in figure 1.2 summary histograms of meteorological conditions (1-minute mean wind speed and 10-minute significant wave height) over the entire cruise. We note in passing that the cruise mean wind speed was 11.3 m/s and that for 23% of the cruise, the wind was over 15 m/s. Cruise mean Hs was 4.6 m with recorded maxima in excess of 13 m ! For more information on shipboard meteorological systems, see Yelland and Kent, in the cruise report.

The next section of this report presents the ACCP data and related measurements; the final section offers some summary comments.

2. DATA

2.1 Processing

The data processing method was similar to that reported for the ACCP on RRS *Discovery* cruise 214 in Griffiths *et al.* (1995). The most important change was the addition of a gyro compass interface with the ACCP electronics so that a continuous real-time heading record was available. The functions of the processing execs are summarised below. Initial experimentation in different weather conditions suggested that depth penetration of the ACCP profiles did not much depend on the type of depth resolution chosen. We fairly arbitrarily kept to the 'coarse' setting for all data recording, the depth bins for which are given in table 1 below. The ping rate was approximately 0.1 Hz, so we chose 10 minute intervals for binning.

Table 1: Bin depths for ACCP coarse resolution setting.

Bin	Depth (m)	Bin	Depth (m)
1	68.9	10	640.6
2	120.2	11	722.8
3	175.2	12	810.2
4	233.0	13	903.6
5	293.0	14	1003.7
6	355.6	15	1111.2
7	421.3	16	1226.9
8	490.3	17	1351.4
9	563.2	18	1485.4

Summary of execs:

CSEXEC0: read ACCP ascii data into pstar; convert time in year / month / day / hour / minute / second into time in seconds from reference time.

CSEXEC1: correct PC clock drift.

CSED1.exec: delete partial data columns from end of file (this results from halting recording while the PC is still processing a 'ping'); recalibrate heading to degrees from hundredths of degrees and depth to metres from decimetres; where flag VALID = 0, set data to absent.

CS2.exec: correct gyro headings with Ashtech 3DF GPS headings.

CSBIN.exec: bin ACCP data on time (10 minute bins) and calculate %good for bins. Also scale water velocities from mm/s to cm/s, and swap signs of eastwards and northwards components to conform with convention.

CS4.exec: merge ACCP relative water velocity with differential GPS ship velocity (smoothed to 10-minute time scale to conform with ACCP data) to calculate absolute current velocity.

Note that the usual relative water velocity amplitude and heading calibrations are absent from this processing. It had been intended to detemine the heading correction using bottom-track data but two separate problems, one of data replay and one of bottom-track velocity initialisation, meant that no bottom track data were recorded on the cruise. The first problem was fixed by new software sent by RDI to Reykjavik for collection during the mid-cruise port call, but this merely served to make the second problem apparent. This omission is not too important for the type of analysis discussed here, but will be further mentioned below.

The four data segments, numbers 2 to 5, are presented in figures 2 to 5. Segment 2 is a little over half a day long; segment 3 covers 2 days; segment 4 a little over a day and a half; and segment

5 a little under four and a half days. There are four panels of data for each 24-hour period covering the data segments. The first panel shows %good contoured versus time and depth; the second panel shows 1-minute mean wind speed and 10-minute Hs; the third and fourth panels show the contoured standard deviation (sd) of north and east components of water velocity measured by the ACCP, versus time and depth, and the sd of the north and east components of ship velocity over the ground measured by differential GPS. Note that the %good plots appear different from the sd plots because where VALID = 0, currents are absent and so not plotted but %good = 0 and so are plotted. These plots also show a time line to indicate when the ship was on station. Station number is shown below a three-pronged symbol that represents quite well for CTD stations the start down, at bottom and end at surface times for the cast. Periods of towing SeaSoar are shown.

2.2 General observations

We proceed with some general observations, in no particular order, on the data presented in figures 2 to 5.

2.2.1 Near-surface absent data. As has been previously observed (Griffiths *et al.*, 1995), no good data are returned from approximately the top 200 m of the water column. GBM suggest the cause to be an acoustic resonance ('ringing') within the vessel triggered by the ACCP ping which masks the ACCP return signal. Subsequent investigation (Griffiths, 1999, pers. comm.) has narrowed down the location of resonating chamber to an oil tank adjacent to the ACCP housing.

2.2.2 Maximum data return layer. In all cases, the maximum data return, up to 95 %good, occurs roughly between 200 and 600 or 700 m. Good data begin immediately below the top noisy level described above, and there is usually a similarly sharp drop-off at the lower limit. Both upper and lower limits change from <10 %good to >75 %good over about 100 m.

2.2.3 Multiple maxima. There is not always a single maximum return layer. On occasion we see multiple maxima with depth: eg, segment 4 day 1 (figure 4.1), where there appear to be 2, 3 or even 4 layers of 'good' data separated by zero or near-zero returns.

2.2.4 On-station increase of data return. It can be seen in segment 2 (figure 2) and elsewhere that while the ship is near-stationary on CTD stations that there is a marked enhancement of the depth range of ACCP signal return, and that this enhancement conforms to a consistent pattern. Firstly, we see data from as far down as the limit of the ACCP's range - 1485.4 m in this case. Secondly, this enhanced return occurs in a three-pronged form: high return at the start of the station, again when the CTD is at the bottom, and again at the end of the station. These three periods are separated by low or zero returns. This tends to confirm the implications of GBM's

observation of the CTD winch as source of acoustic noise. With the ship stopped and the winch at rest, in calm weather, the ACCP can function as specified. When the winch is operating, to lower or raise the CTD, it appears that noise from the winch can mask the ACCP signal return, even in calm weather.

2.2.5 Appearance of the bottom. There are several instances of the bottom topography appearing in the ACCP water-track data return: eg, segment 3 day 1 (figure 3.1) on the approach to the south coast of Iceland, segment 5 day 3 (figure 5.3) on the approach to Cape Farewell, and elsewhere.

2.2.6 Zero data in severe weather. The onset of severe weather reduces data to near zero at all depths. See in particular segment 5 days 4 and 5 (figures 5.4 and 5.5), when during a long SeaSoar tow, with the ship travelling at about 8 knots on a steady heading, the wind speed rose quite quickly to about 16 m/s, followed by the slower rise of wave height to Hs over 5 m. The data return peters out during this period with the top of the maximum return layer remaining around 150 - 200 m, the bottom of the layer rising slowly from 600 to 400 m, and the central maximum %good reducing from over 95% to generally less than 25%. There are other examples.

2.2.7 Ship manoeuvring and velocity sd's. Ship manoeuvres for arriving and departing station, deploying and recovering SeaSoar etc. are clearly visible in computed sd's of all velocity components – both ACCP measured water velocities and GPS measured ship velocities; see third and fourth panels of all figures 2 to 5. It takes the ship about 10 minutes to come on station, ie, to slow down from passage speed (4-5 m/s or 8-10 knots) to near-zero speed. The one or two 10-minute bins covering these periods have velocity sd's of about 200 cm/s, as expected. The GPS velocity spikes off the top of the plots are of this magnitude.

2.2.8 Background velocity sd's. The modal ACCP relative water velocity sd's are 26-28 cm/s. The modal GPS absolute ship velocity sd's are 6-8 cm/s. The cruise report shows that the differential GPS positions are accurate (±3 sd's) to ±2 m. Over 10 minutes, this is equivalent to a velocity error of 0.3 cm/s. Similarly, Ashtech headings are accurate to about 0.1°, equivalent to a 10-minute velocity error of 1 cm/s. Therefore the ship velocity sd's are caused by real velocity variations, not by navigational error; and further, the dominant error in calculating absolute water velocities is that due to ACCP relative water velocity measurements.

2.3 Functional dependence of %good

In figure 6, we show the dependence of %good on depth and wind speed (figure 6.1), depth and Hs (figure 6.2), depth and relative wind direction (figure 6.3), and depth and ship speed (figure 6.4). We show the distributions of %good (first panel), sd(%good) (second panel), histogram of

occurrences of independent variable (third panel), and standard error (se) per bin of independent variable (fourth panel).

2.3.1 Wind speed. Features identified above are summarised here. There is a maximum return layer between about 200 and 600 m, in which %good decreases with increasing wind speed. In this band, the lowest variance of %good is associated with highest %good, and *vice-versa.* The high wind speed, high %good return is rather anomalous, being based on very few values with very high sd. The low wind speed, deep returns are from the on-station periods. There is a suggestion of an effective cut-off in data return at about 16 m/s.

2.3.2 Significant wave height. This distribution is similar to that of wind speed. The cut-off appears at Hs = 6 m.

2.3.1 Relative wind direction. Here, the directions 0° and 360° are ahead, 180° is astern, 90° is starboard and 270° port. There is no obvious preferred relative wind direction. Enhanced %good centred on 190° results from rather few measurements, so although one might expect a reduced bubble layer under the ship with a following wind, thus reducing interference with the ACCP signal, the evidence here is inconclusive.

2.3.4 Ship speed. Ship speeds are clustered around 0 (on-station), 4 m/s (8 knots, SeaSoar tows) and 6 m/s (12 knots, on passage). The reasons for the low speed enhancement are obvious. The reasons for the reduced %good about 3.75 m/s and the increased %good on passage are not so obvious; they are probably convoluted with meteorological conditions.

2.4 Comparison with acoustic Doppler current measurements

There are two other sources of current measurements on the cruise, both acoustic Doppler current profilers (ADCPs): the vessel-mounted ADCP (VM-ADCP), measuring continuously both underway and on station, and the lowered ADCP (L-ADCP), making surface to bottom current profile measurements on station. See the cruise report for further information. We must first check that, in the absence of a proper calibration for the ACCP water velocity measurements, that those measurements are at least close to correct in direction and magnitude.

2.4.1 ACCP water velocity and GPS ship velocity comparisons. In order to confirm that we have the ACCP current components at least nearly the right way round and of nearly the right magnitude, we show in figure 9 the ship velocity over the ground derived from differential GPS plotted against the ACCP-measured water velocity relative to the ship. There should be a 1:1 relationship between the GPS and ACCP components, with a slope of -1 for reversal of sense, assuming zero mean currents so that there is no overall bias in ACCP water velocities. The fit statistics are given in Table 2 below.

Table 2: Fit statistics for differential GPS ship velocity components (Ve-S and Vn-S) versus ACCP water velocity components (Ve-A and Vn-A), where e and n stand for east and north. X and Y are dependent and independent variables per fit.

X	Y	slope	offset (cm/s)	r^2
Ve-S	Ve-A	-0.9959	-6.064	0.9796
Vn-S	Vn-A	-0.9890	-1.024	0.9760

It is apparent that there is a very good fit here, so we can proceed with some confidence to inspect ACCP currents.

2.4.2 On-station comparisons. We choose two stations to compare absolute currents between ACCP (10-minute ensembles), VM-ADCP (2-minute ensembles) and L-ADCP. The first station (12942) occurred during ACCP data segment 2 (see figure 2) in fairly good weather. The second (12985) occurred during segment 4 day 2 (figure 4.2) in poor weather. Both managed deep penetration, to over 1200 m. North and east current components are shown for both stations and all three instruments in figure 7. The absence of ACCP data from the top 200 m is a hindrance here. On station 12942 (fig. 7.1) there appears to be a small (~5 cm/s) mismatch between the L-ADCP and the other two. Most notably, the ACCP current profiles increase in scatter with depth; each profile is already a 10-minute ensemble with current sd's ~25 cm/s. Furthermore they appear to diverge from the L-ADCP profiles below about 800 or 900 m. The ACCP profile scatter is ±20 cm/s below 900 m on station 12942 in fair weather, but is about ±50 cm/s on station 12985 (fig. 7.2) below 900 m in poor weather. Both divergence and scatter are disappointing.

2.4.3 Underway comparisons. We want to compare underway VM-ADCP currents with underway ACCP currents. We form 10-minute means of the 2-minute VM-ADCP ensembles so both data sets match in time. There is not much overlap in depth so we choose to compare at a single ACCP level: 356 m, bin 6. This bin is about 64 m wide, so we average the VM-ADCP data with depth over bins 40-48 on 4 m depth resolution: ie 356 ± 32 m. Figure 8 shows the results of plotting VM-ADCP vs. ACCP currents for east and north components for all data and for data subselected for low (< 1 knot, 0.5 m/s) ship speed and for high (<8 knot, 4 m/s) ship speed, with plots on wide and narrow current ranges. Table 3 below shows fit statistics.

Table 3: Fit statistics for VM-ADCP current velocity components (Ve-ADCP and Vn-ADCP) versus ACCP current velocity components (Ve-ACCP and Vn-ACCP), where e and n stand for east and north. X and Y are dependent and independent variables per fit. 'Slow' and 'Fast' refer to ship speed as above.

Ship speed	X	Y	slope	offset (cm/s)	r^2
Slow	Ve-ADCP	Ve-ACCP	0.9937	-0.2326	0.5467
	Vn-ADCP	Vn-ACCP	0.9552	0.3617	0.5520
Fast	Ve-ADCP	Ve-ACCP	1.1010	-1.4678	0.5430
	Vn-ADCP	Vn-ACCP	1.1416	6.4798	0.5358

Plainly the results are mixed. For on-station data, the VM-ADCP and ACCP currents are very similar; it appears that ACCP currents are about 0.5% low compared with VM-ADCP. The picture is different underway however, where ACCP currents now appear to biased high by 10-15%. There is much scatter: r^2 is ~0.55, and ACCP current variances are double the VM-ADCP variances. It is possible that the large bias under 'fast' is a consequence of the lack of calibration of the ACCP. With current sd's about 10 cm/s at 356 m, it only needs 0.1° heading error to introduce a 1 cm/s bias over 10 minutes, so without further analysis, we cannot be sure of the cause of the bias.

3 FINAL COMMENTS

The ACCP was not much fun to operate on a foul-weather cruise, because it simply returned no good data for days on end in the worst of the weather. Even by recording data during relatively placid periods, the data return was still rather poor. Some of the causes of this unfortunate state of affairs have been identified by GBM, particularly the ringing tank and the noisy winch. Nevertheless, it is not clear that either of these impinge on the maximum depth penetration of the instrument while the ship is underway, so it seems possible that environmental noise is a limiting factor in ACCP performance: screening by bubble layers under the ship's hull, sub-surface noise in high wind / wave conditions through wave breaking, bubbles popping, etc. Installation of a bubble deflector shield outside the hull in the way of the ACCP transducer head (GBM again) has not made an obvious difference.

To be a desirable underway current profiling tool, the ACCP needs to offer at least a factor two improvement over the VM-ADCP, which routinely manages 0 - 400 m depths in 2 minute

ensembles and 4 m resolution in all but the worst weathers. At present, if the near-surface problems could be overcome, we might get 0 - 600 m depths in 10 minute ensembles and ~ 60 m resolution in fine to moderate weather. A 200 m increase in depth penetration for an order of magnitude worsening of time and depth resolution combined with a lack of robustness is not worth the bother.

ACKNOWLEDGEMENTS

Thanks to Gwyn Griffiths (SOC-OTD) for advice and Steve Bradley (RDI) for assistance during *Discovery* 223. This study was funded by the SOC Technology Innovation Fund.

REFERENCES

Griffiths, G., B. Dupee, G. Watson, P. Spain and T. Nguyen, 1995: Trials and evaluation of an RD Instruments acoustic correlation current profiler in the Agulhas Current on RRS *Discovery* cruise 214. IOSDL Internal Document, No. 349, 61 pp.

Griffiths, G., S. E. Bradley and G. Murdock, 1999: Factor affecting the performance of a shipboard acoustic correlation current profiler. Proc. IEEE 6th Working Conf. on Current Measurement (in press).

Leach, H. and R. T. Pollard, 1998: *RRS Discovery Cruise 223 28 September – 19 November 1996. Vivaldi '96.* SOC Cruise Report, No. 17, Southampton, 104 pp.

This page is intentionally blank.

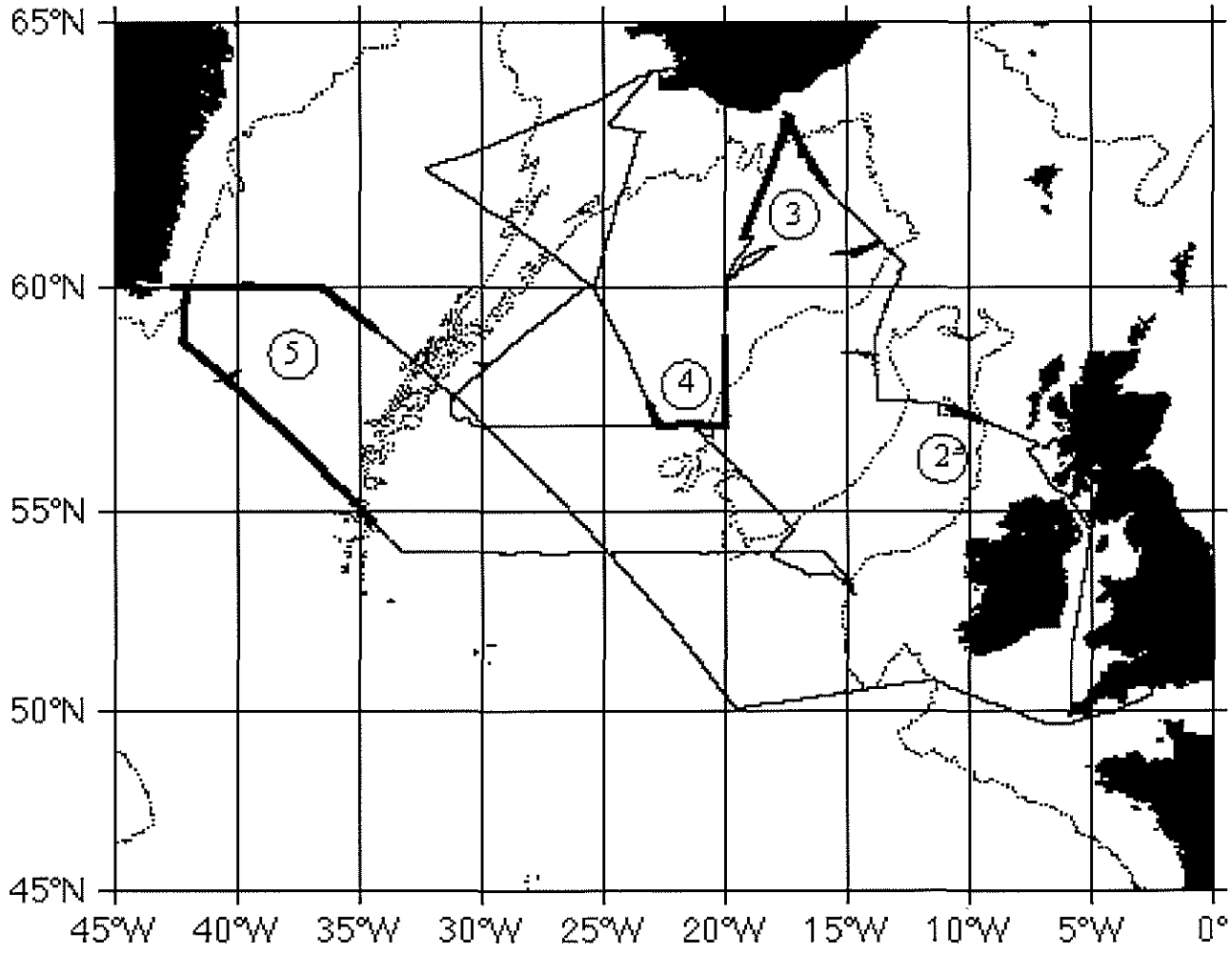

Figure 1.1: Track of RRS *Discovery* during cruise 223. Periods when ACCP data were recorded are shown in bold and numbered 2 to 5. The dotted line is the 1500 m isobath.

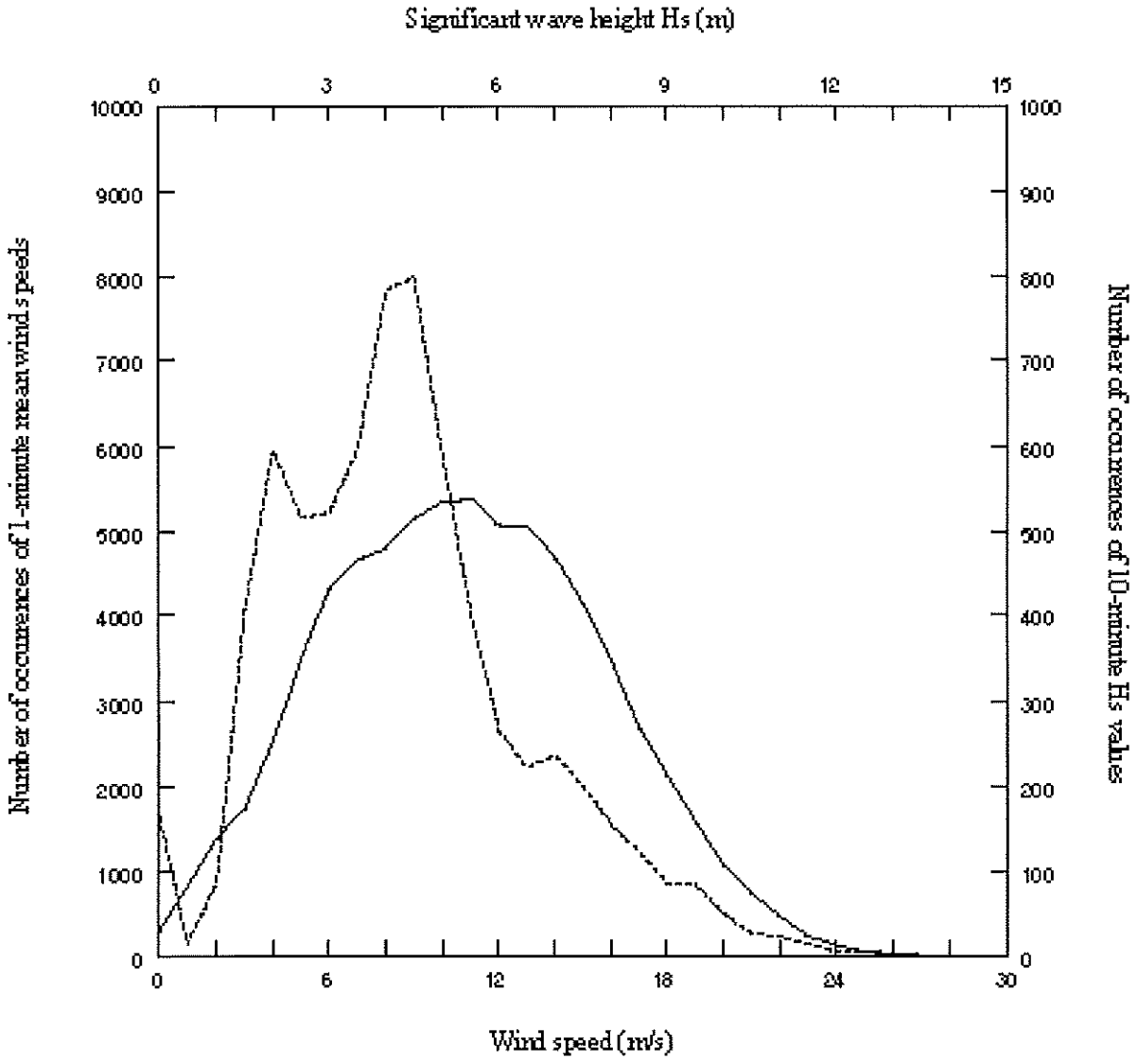

Figure 1.2: Histograms of significant wave height (Hs, m) and wind speed measured throughout *Discovery* cruise 223. Wind speeds are 1 minute means, binned on 1 m/s; Hs estimates are on a 10 minute basis, binned on 0.5 m. Wind speed curve is solid, Hs dashed.

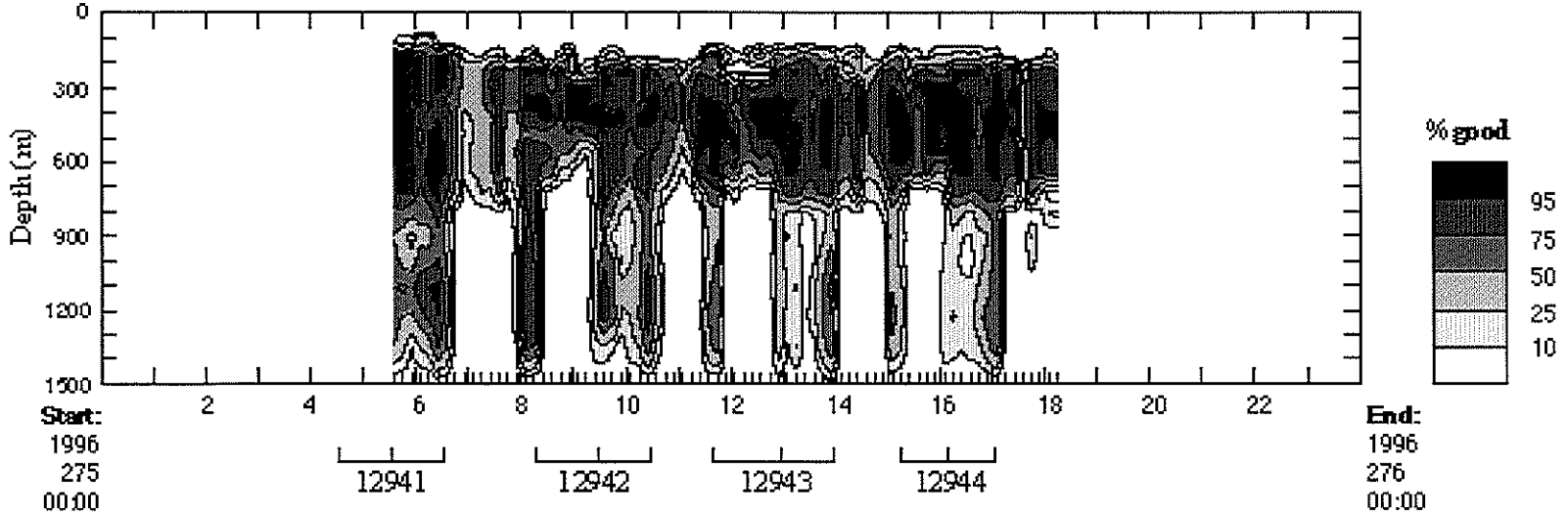

Figure 2.1.1: %good as a function of depth (m) and time (hours). The time axis covers 24 hours; start time (Year - Day - Hours:Minutes [UCT]) and end time (similarly) are shown. Cruise events (CTD stations [5-digit numbers] and SeaSoar tows) are shown on the time line above.

Segment 2

Figure 2.1.2: Significant wave height Hs (solid, left scale) and wind speed (grey, right scale) vs. time.

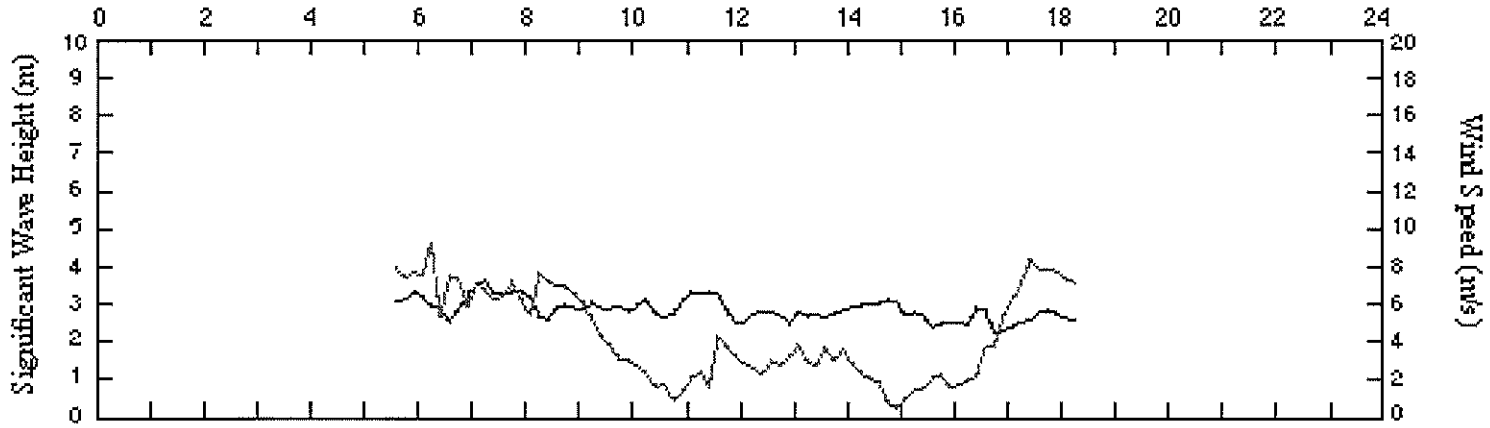

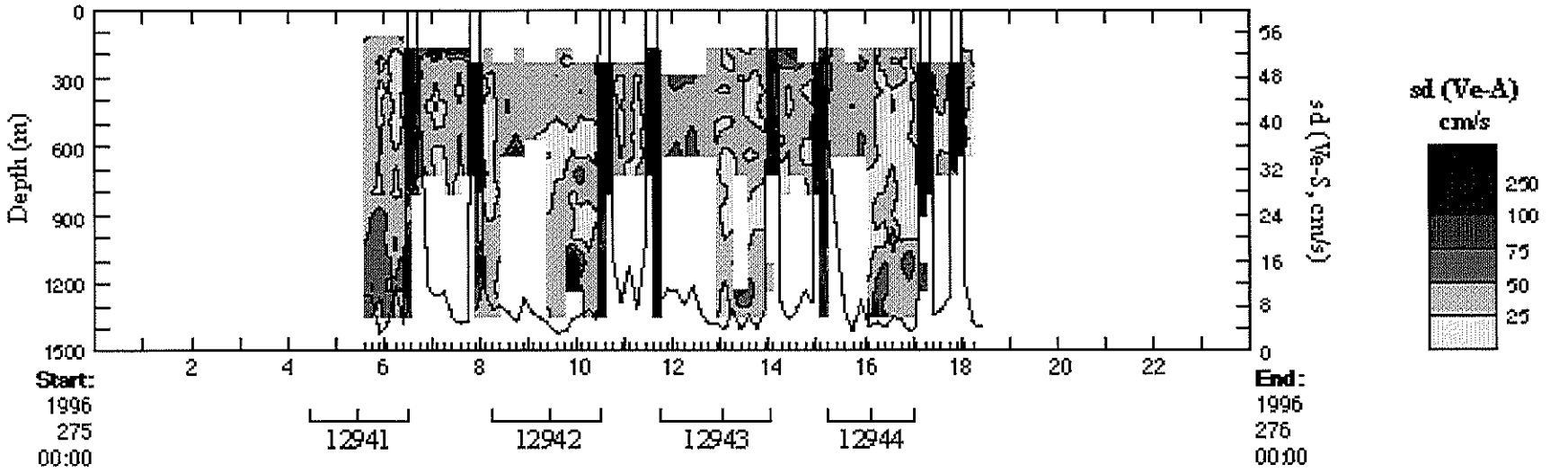

Figure 2.1.3: Standard deviation of east component of water velocity measured by ACCP [sd(Ve-A), contours], and standard deviation of east component of ship velocity over ground measured by differential GPS [sd(Ve-S), solid line, right scale].

Segment 2

Figure 2.1.4: As above, for standard deviation of north velocity components: sd(Vn-A) and sd(Vn-S).

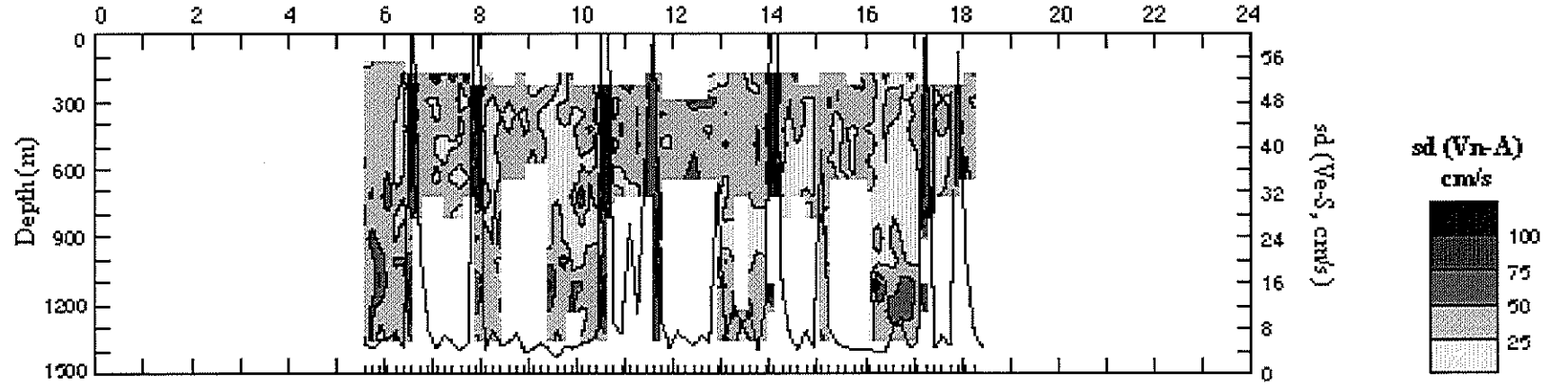

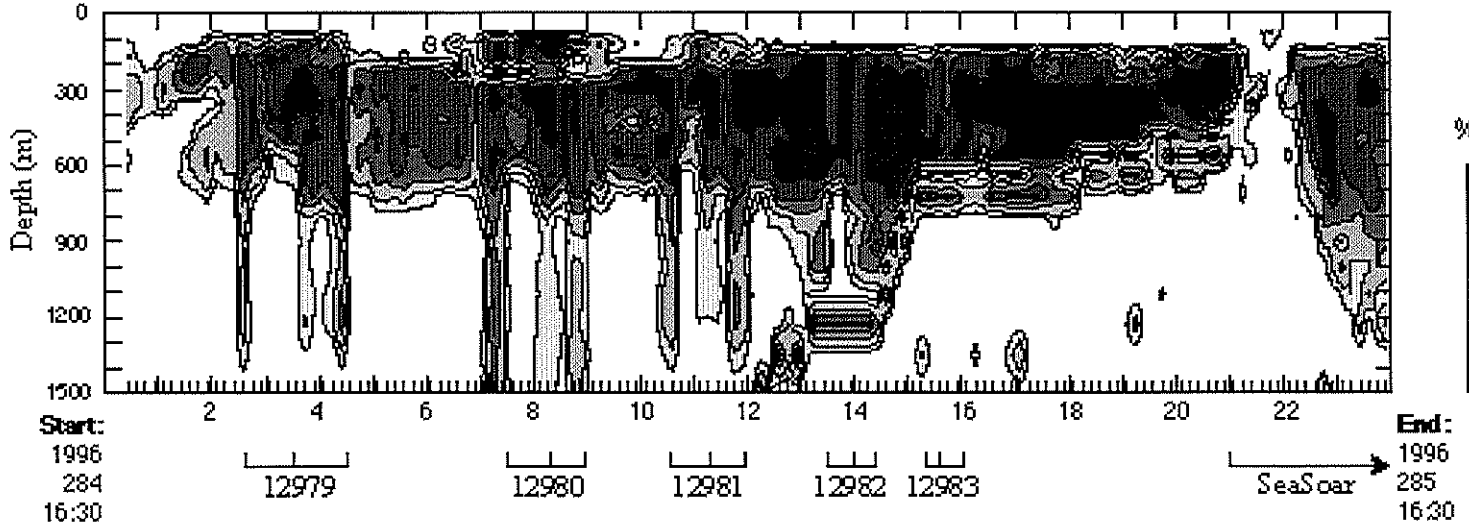

Figure 3.1.1: %good as a function of depth (m) and time (hours). The time axis covers 24 hours; start time (Year - Day - Hours:Minutes [UCT]) and end time (similarly) are shown. Cruise events (CTD stations [5-digit numbers] and SeaSoar tows) are shown on the time line above. The bottom depth encroaches on ACCP range on stations 12982 (depth 1179 m) and 12983 (678 m) and subsequently.

Segment 3 Day 1

Figure 3.1.2: Significant wave height Hs (solid, left scale) and wind speed (grey, right scale) vs. time.

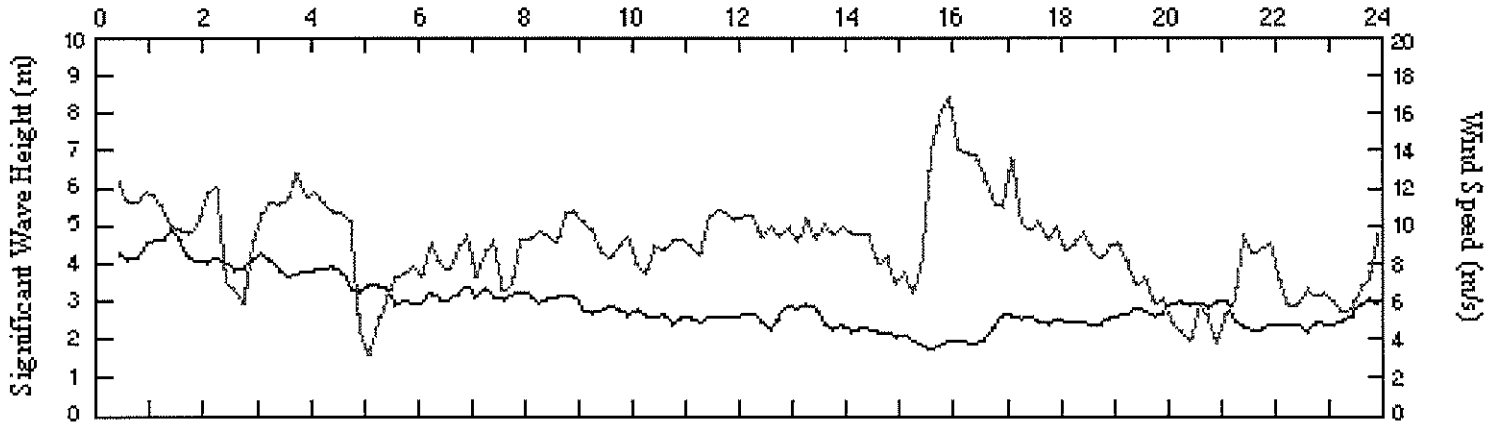

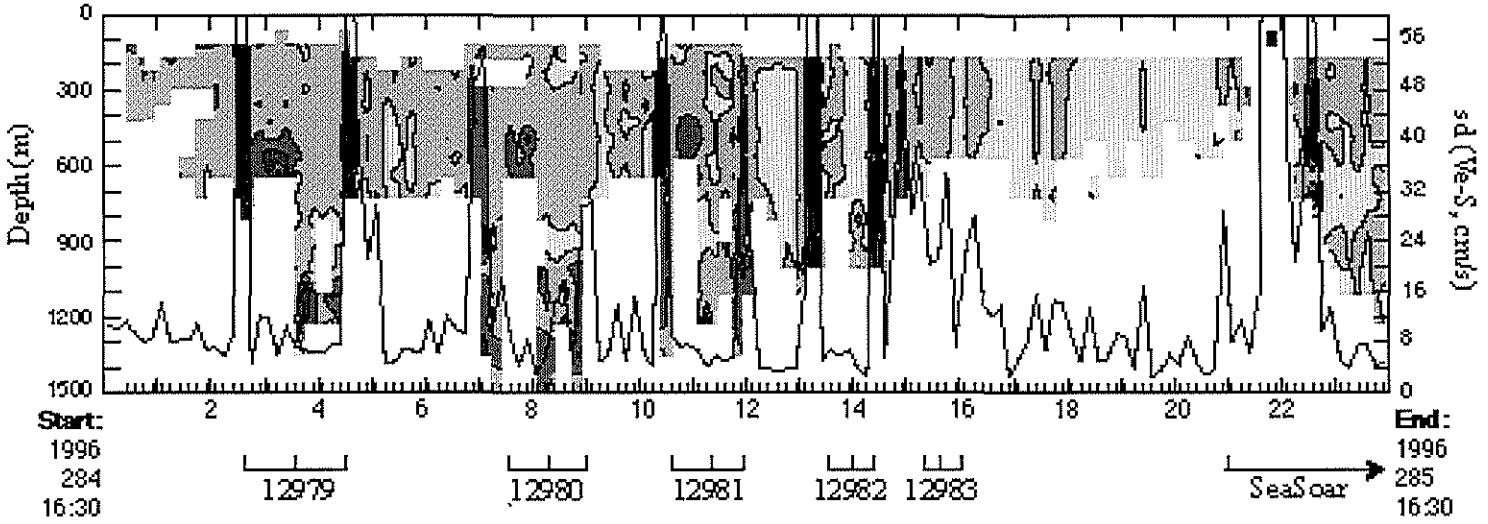

Figure 3.1.3: Standard deviation of east component of water velocity measured by ACCP [sd(Ve-A), contours], and standard deviation of east component of ship velocity over ground measured by differential GPS [sd(Ve-S), solid line, right scale]. Time axis as before.

Figure 3.1.4: As above, for standard deviation of north velocity components: sd(Vn-A) and sd(Vn-S).

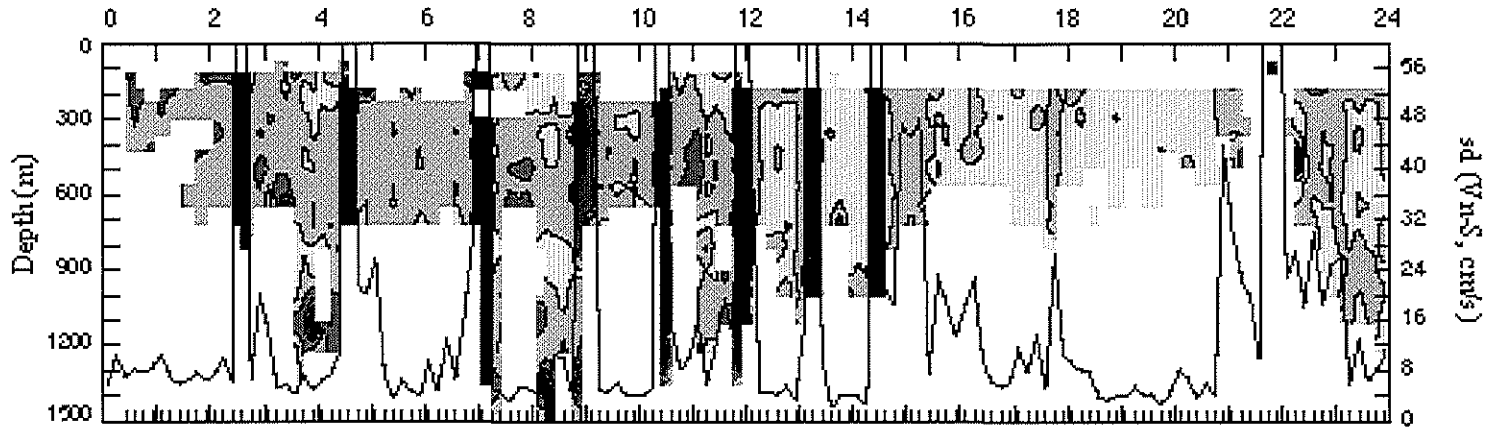

Segment 3 Day 1

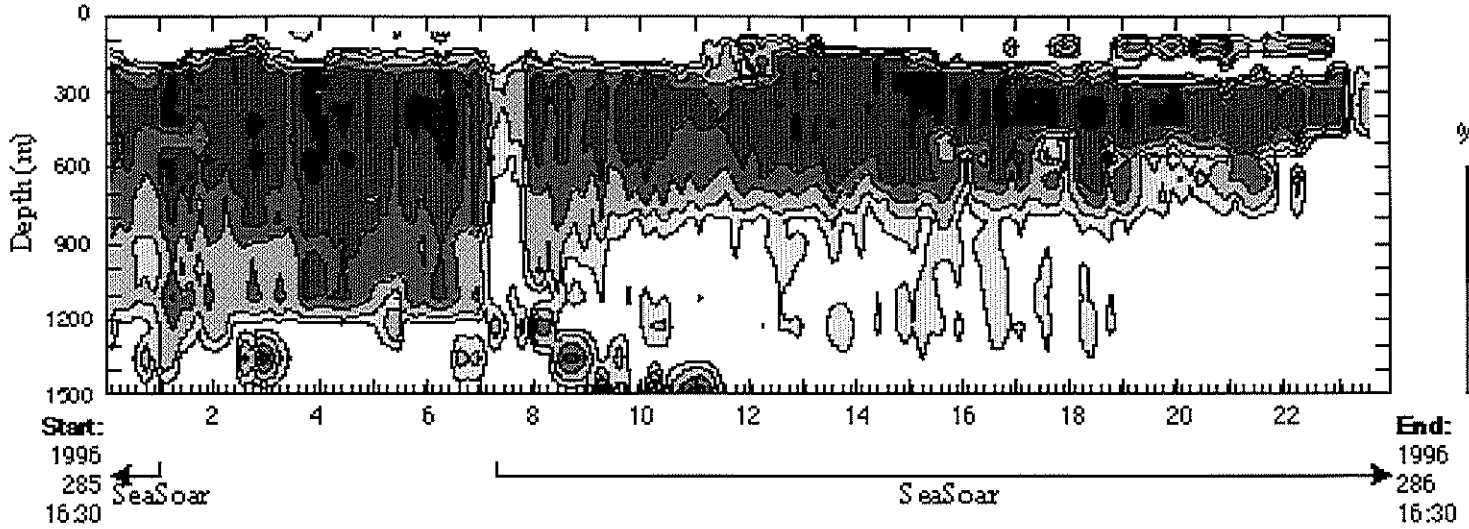

Figure 3.2.1: %good as a function of depth (m) and time (hours). The time axis covers 24 hours; start time (Year - Day - Hours :Minutes [UCT]) and end time (similarly) are shown. Cruise events (CTD stations [5-digit numbers] and SeaSoar tows) are shown on the time line above.

Segment 3 Day 2

Figure 3.2.2: Significant wave height Hs (solid, left scale) and wind speed (grey, right scale) vs. time.

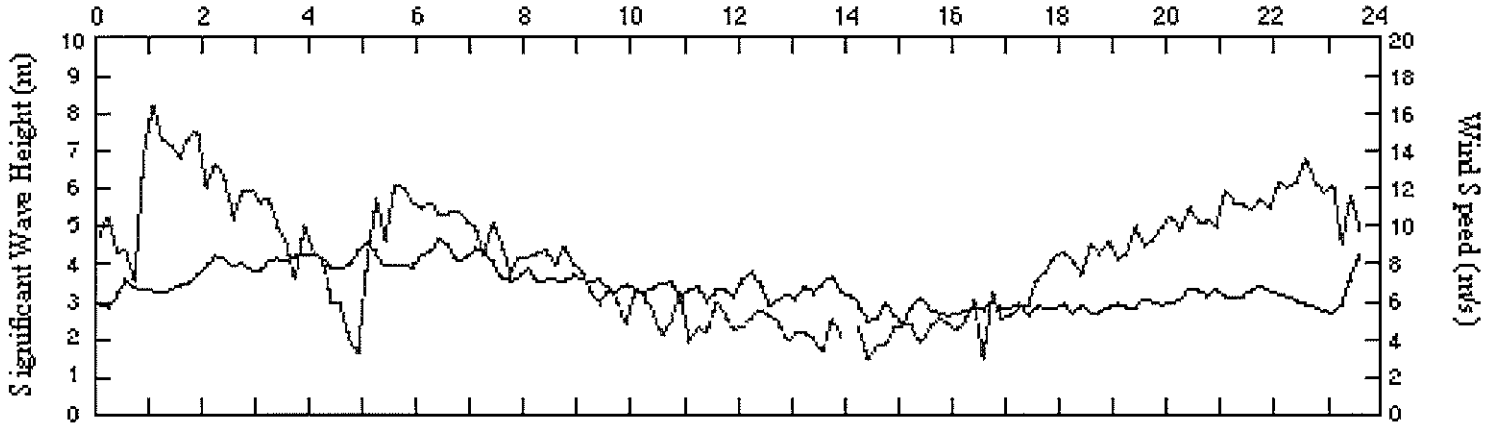

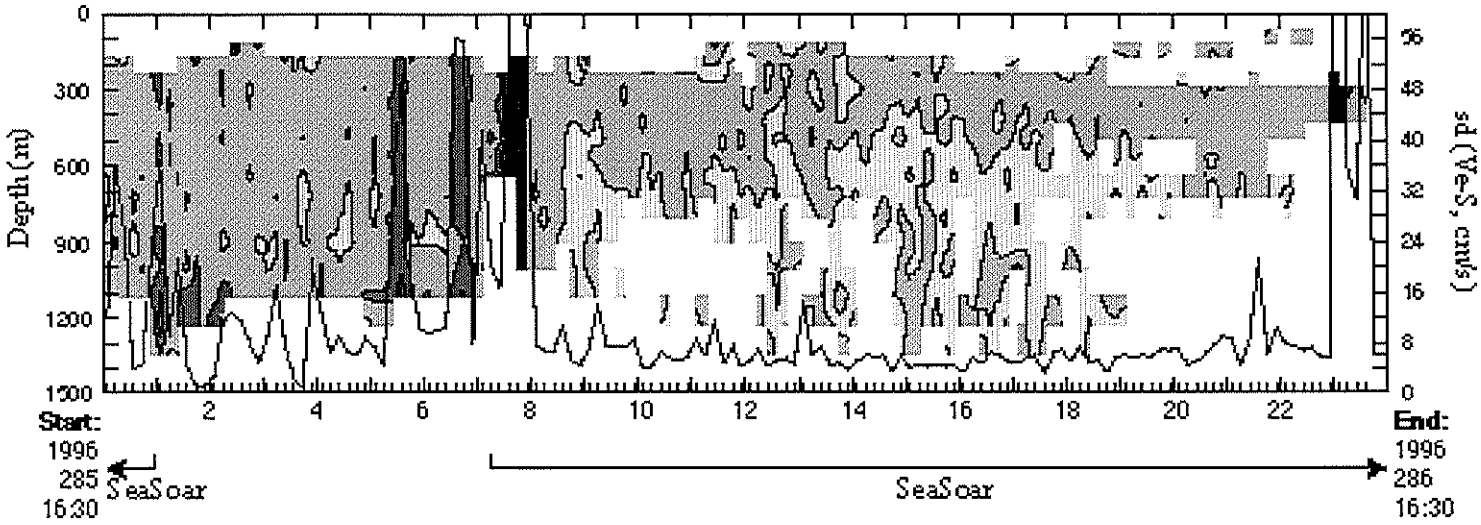

Figure 3.2.3: Standard deviation of east component of water velocity measured by ACCP [sd(Ve-A), contours], and standard deviation of east component of slip velocity over ground measured by differential GPS [sd(Ve-S), solid line, right scale].

Segment 3 Day 2

Figure 3.2.4: As above, for standard deviation of north velocity components: sd(Vn-A) and sd(Vn-S).

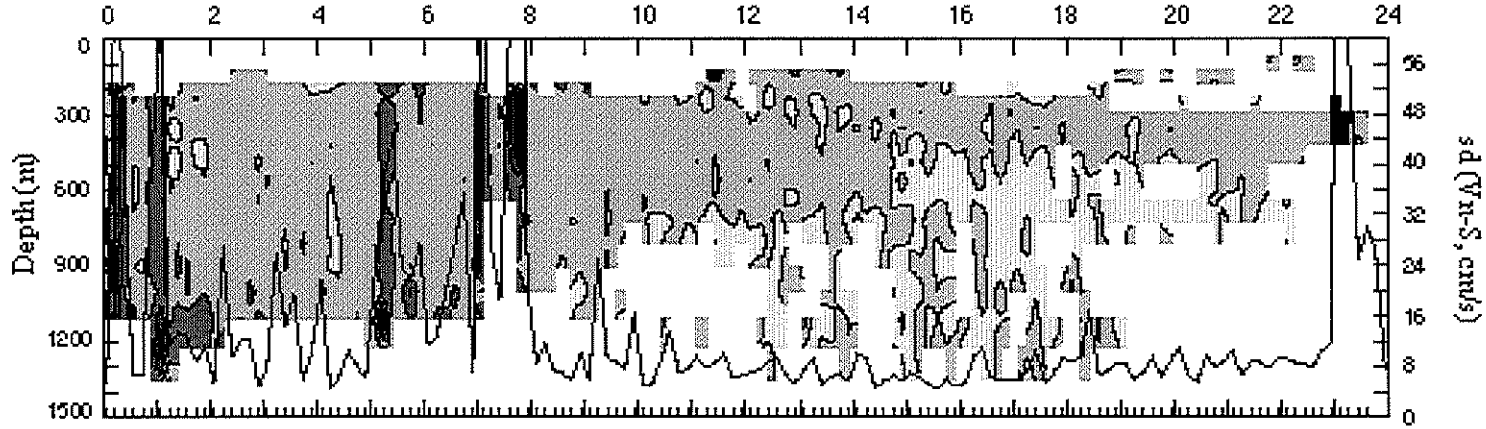

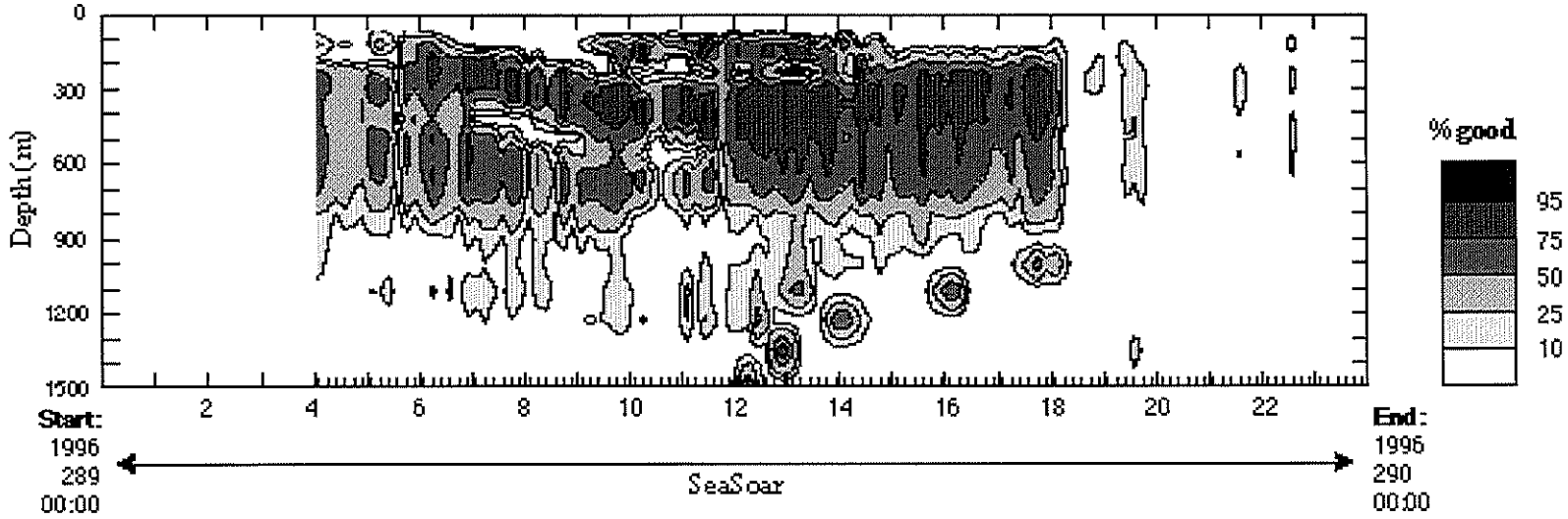

Figure 4.1.1: %good as a function of depth (m) and time (hours). The time axis covers 24 hours; start time (Year - Day - Hours:Minutes [UCT]) and end time (similarly) are shown. Cruise events (CTD stations [5-digit numbers] and SeaSoar tows) are shown on the time line above.

Segment 4 Day 1

Figure 4.1.2: Significant wave height Hs (solid, left scale) and wind speed (grey, right scale) vs. time.

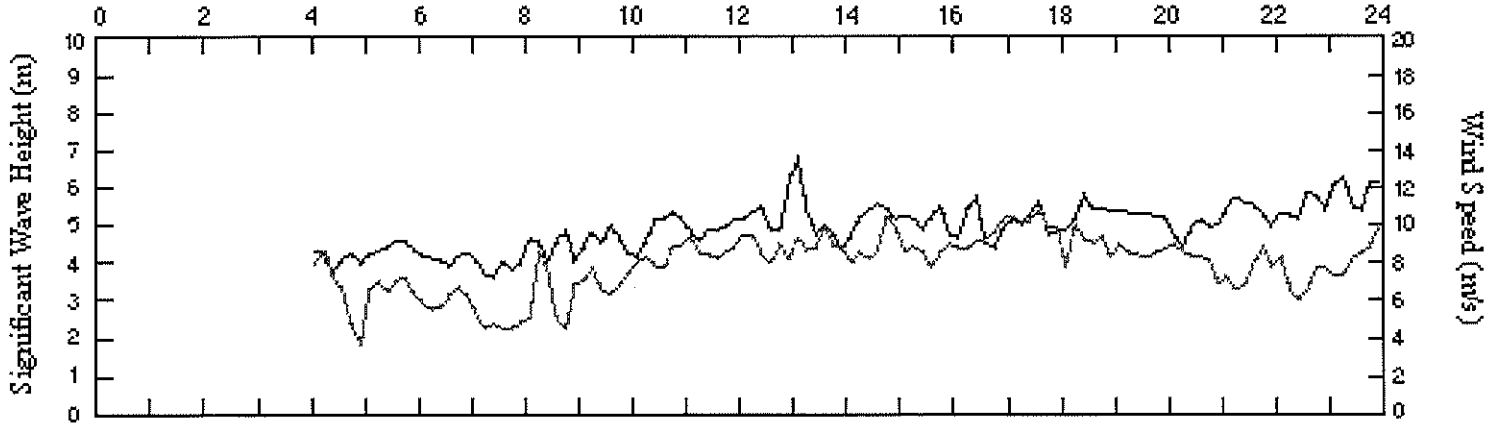

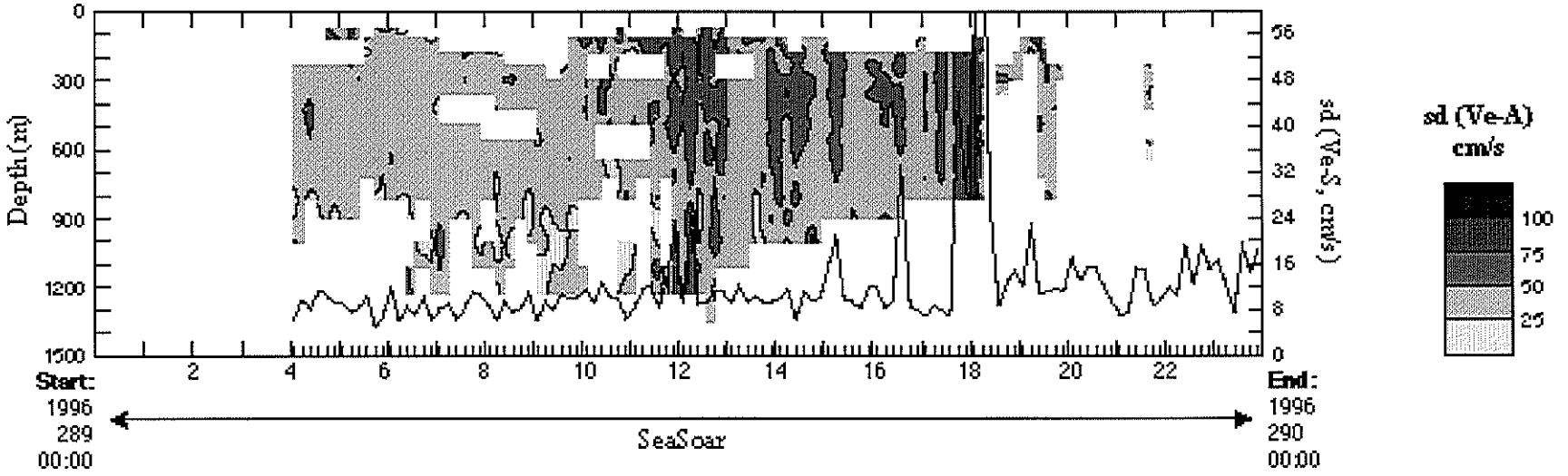

Figure 4.1.3: Standard deviation of east component of water velocity measured by ACCP [sd(Ve-A), contours], and standard deviation of east component of ship velocity over ground measured by differential GPS [sd(Ve-S), solid line, right scale]. Time axis as before.

Segment 4 Day 1

Figure 4.1.4: As above, for standard deviation of north velocity components: sd(Vn-A) and sd(Vn-S).

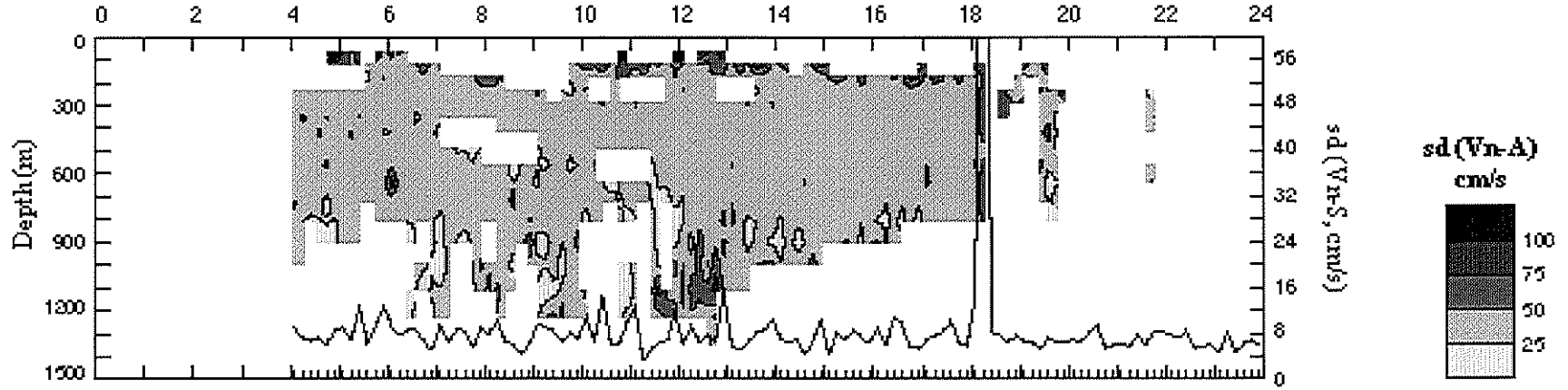

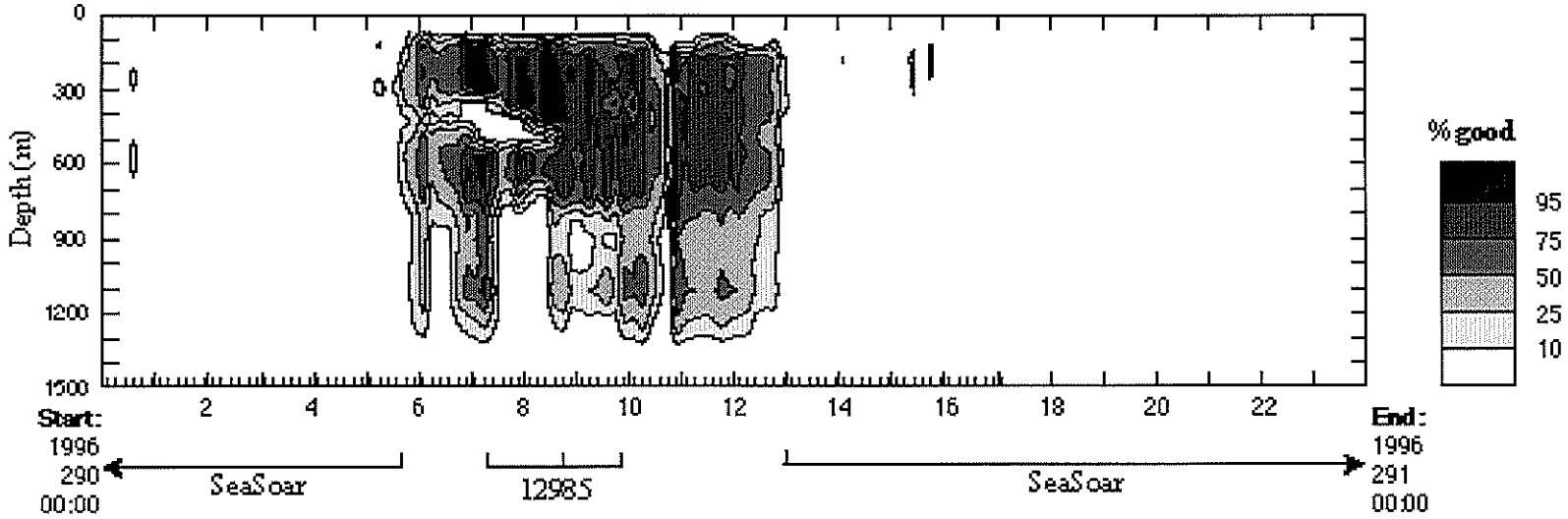

Figure 4.2.1: %good as a function of depth (m) and time (hours). The time axis covers 24 hours; start time (Year - Day - Hours:Minutes [UCT]) and end time (similarly) are shown. Cruise events (CTD stations [5-digit numbers] and SeaSoar tows) are shown on the time line above.

Segment 4 Day 2

Figure 4.2.2: Significant wave height Hs (solid, left scale) and wind speed (grey, right scale) vs. time.

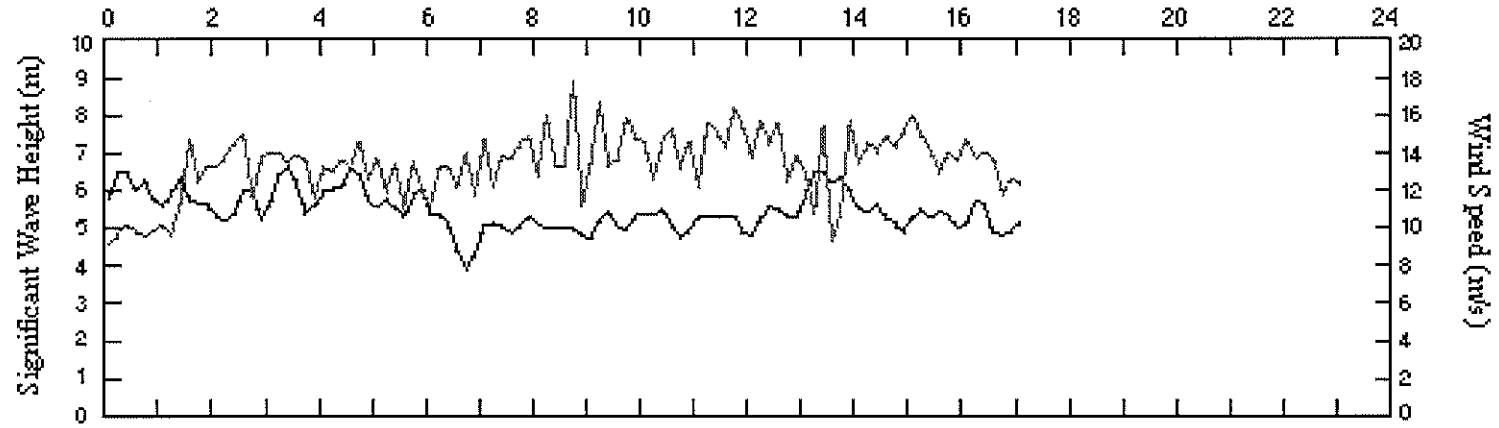

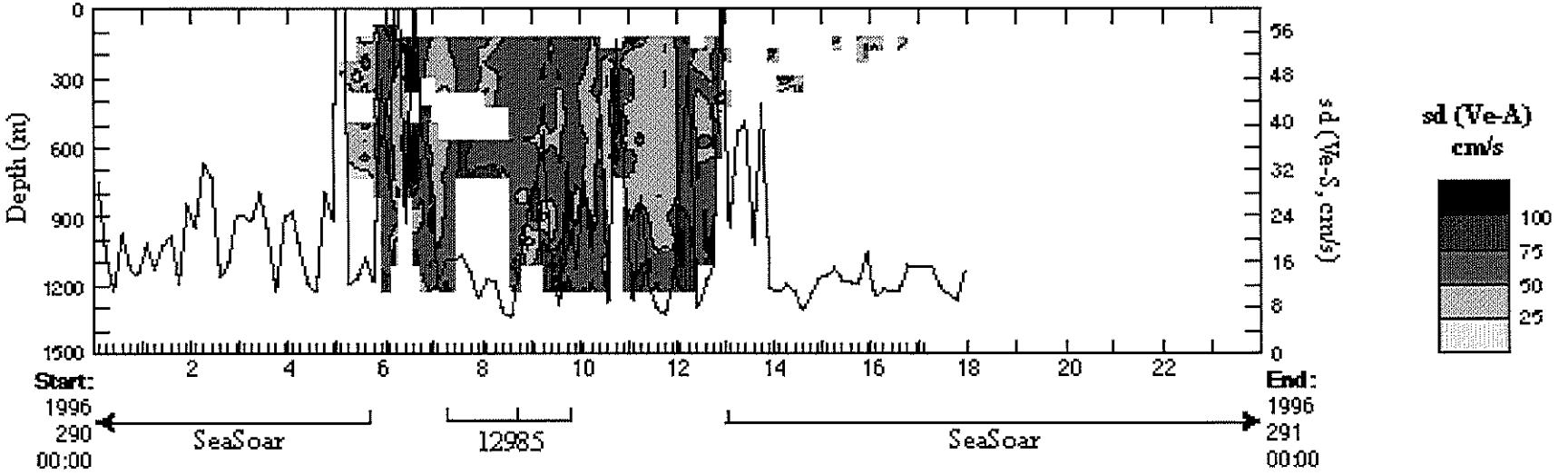

Figure 4.2.3: Standard deviation of east component of water velocity measured by ACCP [sd(Ve-A), contours], and standard deviation of east component of ship velocity over ground measured by differential GPS [sd(Ve-S), solid line, right scale]. Time axis as before.

Segment 4 Day 2

Figure 4.2.4: As above, for standard deviation of north velocity components: sd(Vn-A) and sd(Vn-S).

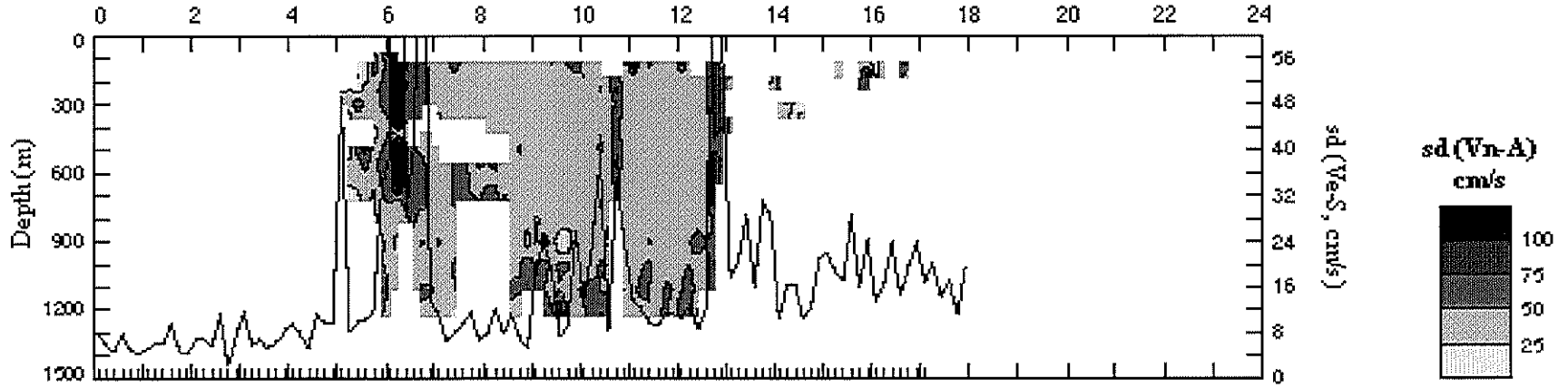

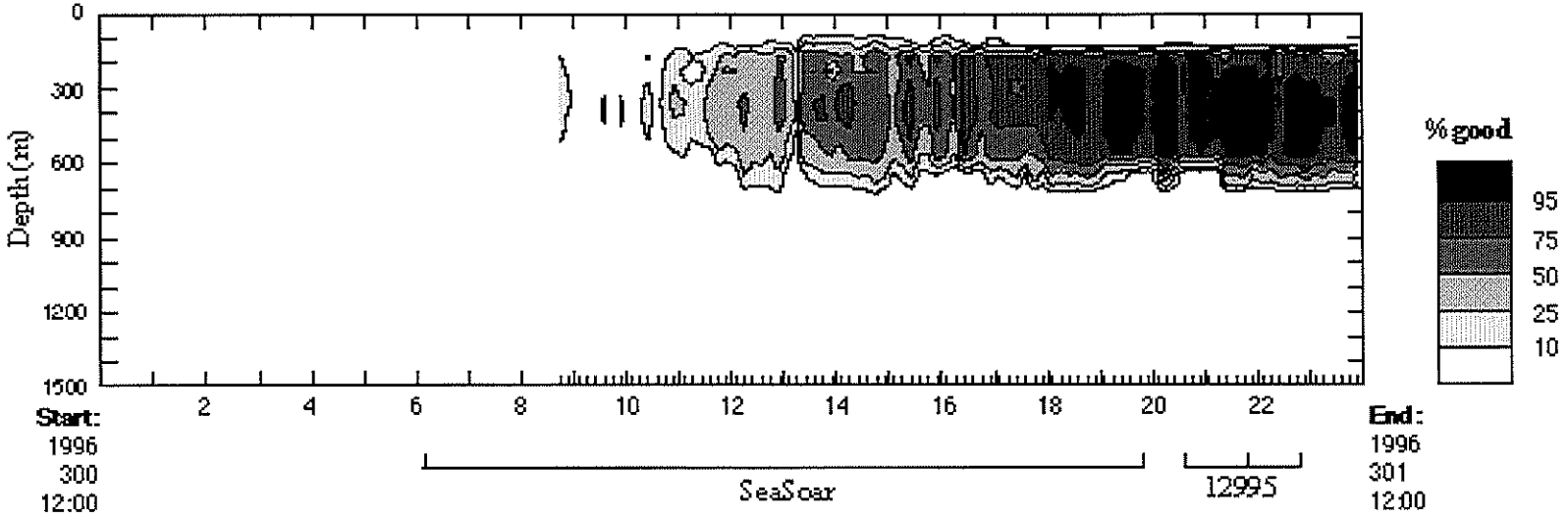

Figure 5.1.1: %good as a function of depth (m) and time (hours). The time axis covers 24 hours; start time (Year - Day - Hours:Minutes [UCT]) and end time (similarly) are shown. Cruise events (CTD stations [5-digit numbers] and SeaSoar tows) are shown on the time line above.

Segment 5 Day 1

Figure 5.1.2: Significant wave height Hs (solid, left scale) and wind speed (grey, right scale) vs. time.

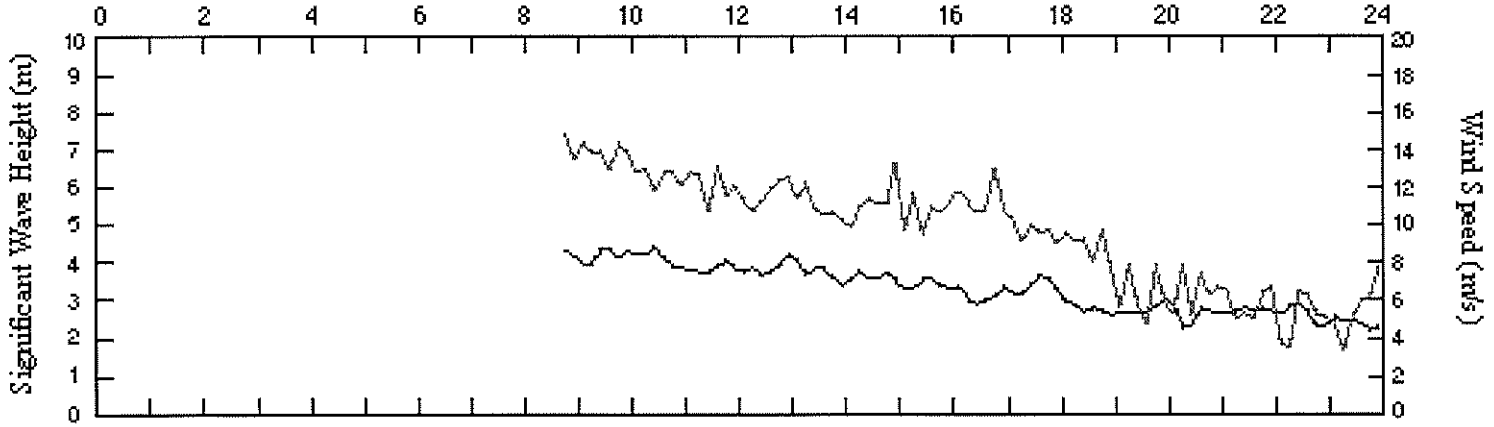

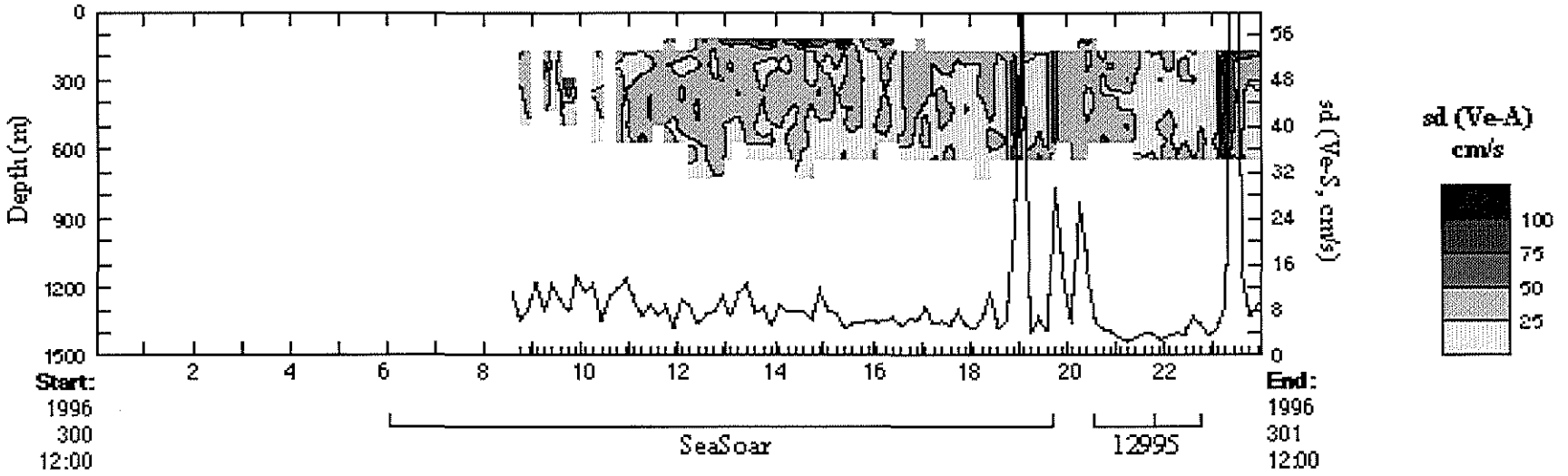

Figure 5.1.3: Standard deviation of east component of water velocity measured by ACCP [sd(Ve-A), contours], and standard deviation of east component of ship velocity over ground measured by differential GPS [sd(Ve-S), solid line, right scale]. Time axis as before.

Segment 5 Day 1

Figure 5.1.4: As above, for standard deviation of north velocity components: sd(Vn-A) and sd(Vn-S).

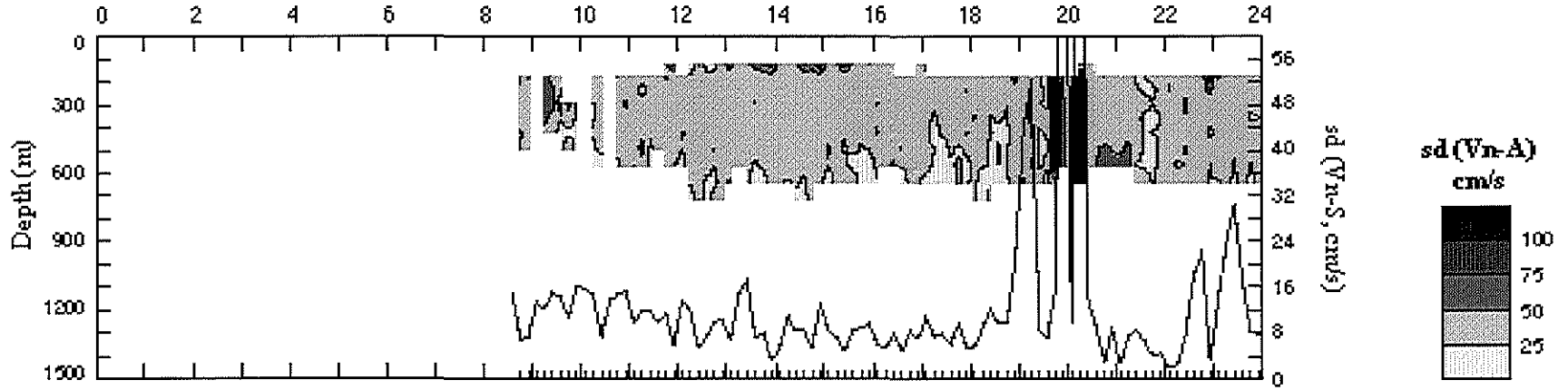

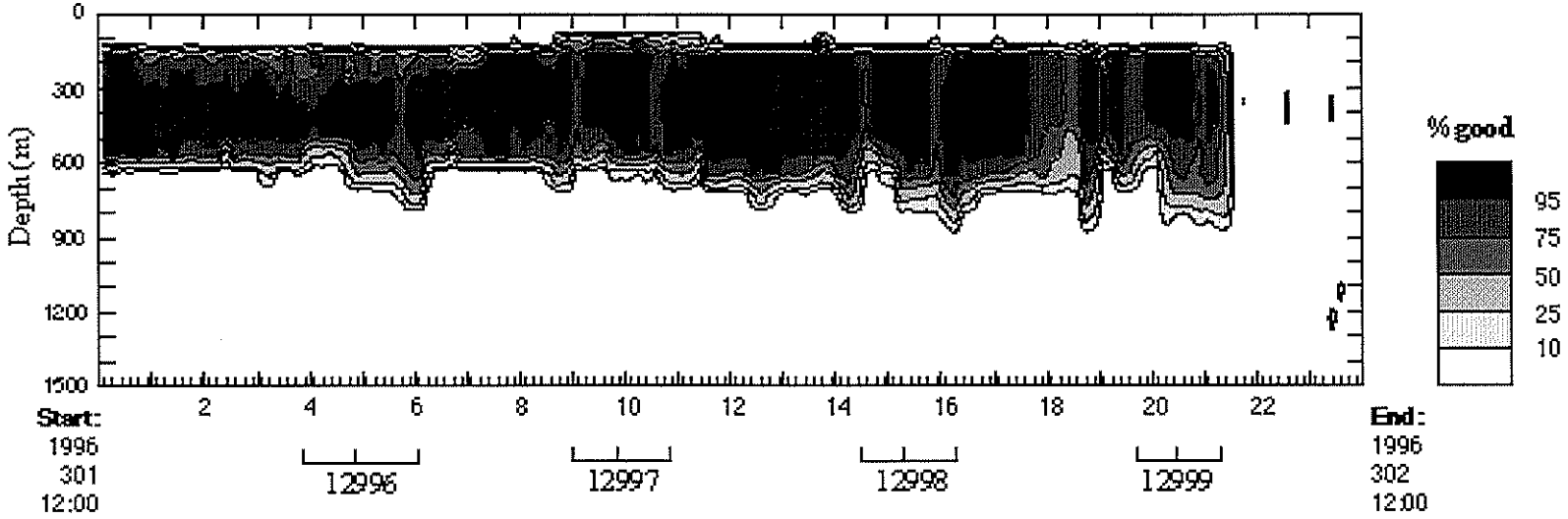

Figure 5.2.1: %good as a function of depth (m) and time (hours). The time axis covers 24 hours; start time (Year - Day - Hours:Minutes [UCT]) and end time (similarly) are shown. Cruise events (CTD stations [5-digit numbers] and SeaSoar tows) are shown on the time line above.

Segment 5 Day 2

Figure 5.2.2: Significant wave height Hs (solid, left scale) and wind speed (grey, right scale) vs. time.

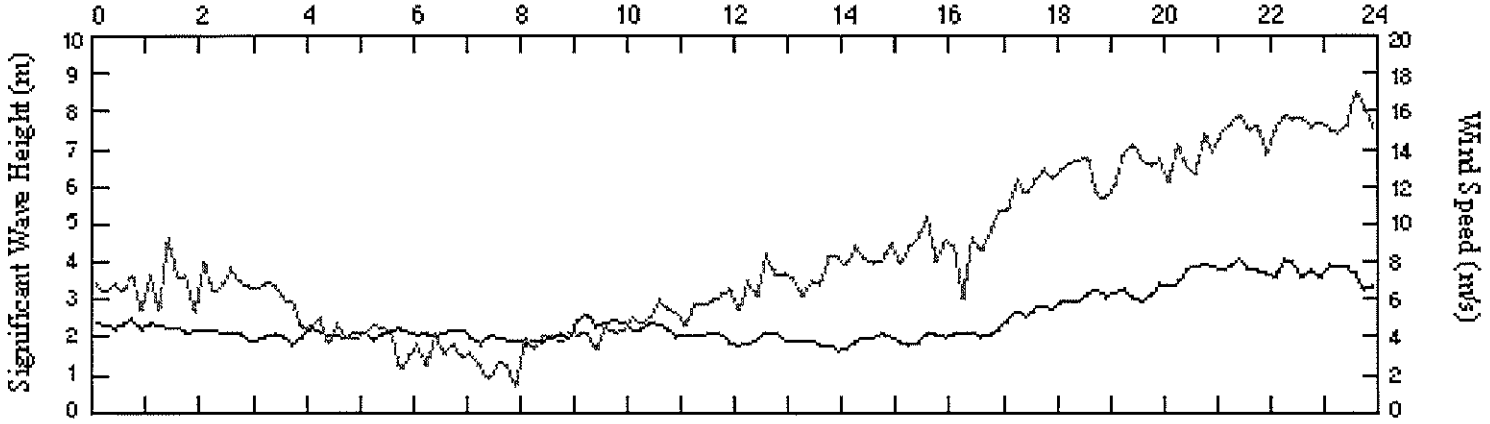

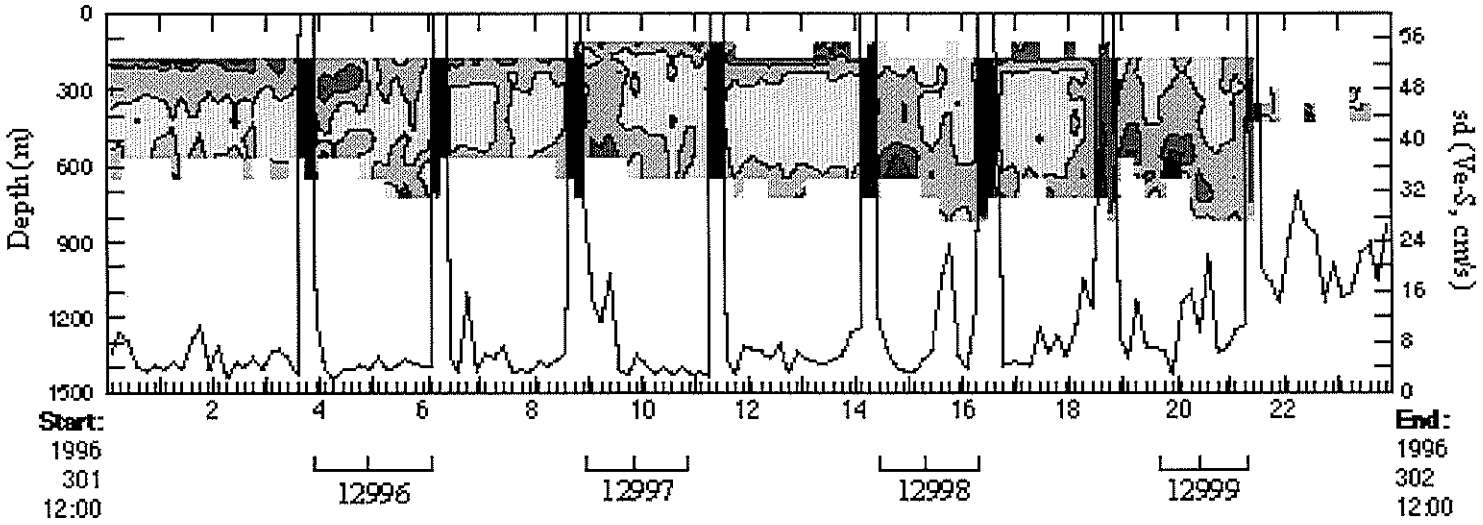

Figure 5.2.3: Standard deviation of east component of water velocity measured by ACCP [sd(Ve-A), contours], and standard deviation of east component of ship velocity over ground measured by differential GPS [sd(Ve-S), solid line, right scale]. Time axis as before.

Segment 5 Day 2

Figure 5.2.4: As above, for standard deviation of north velocity components: sd(Vn-A) and sd(Vn-S).

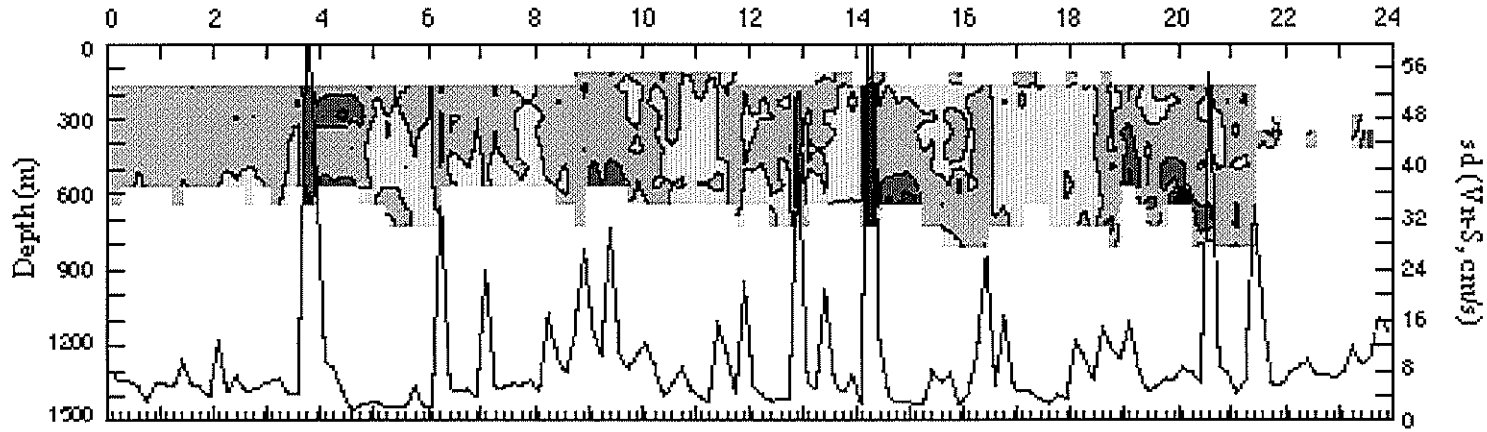

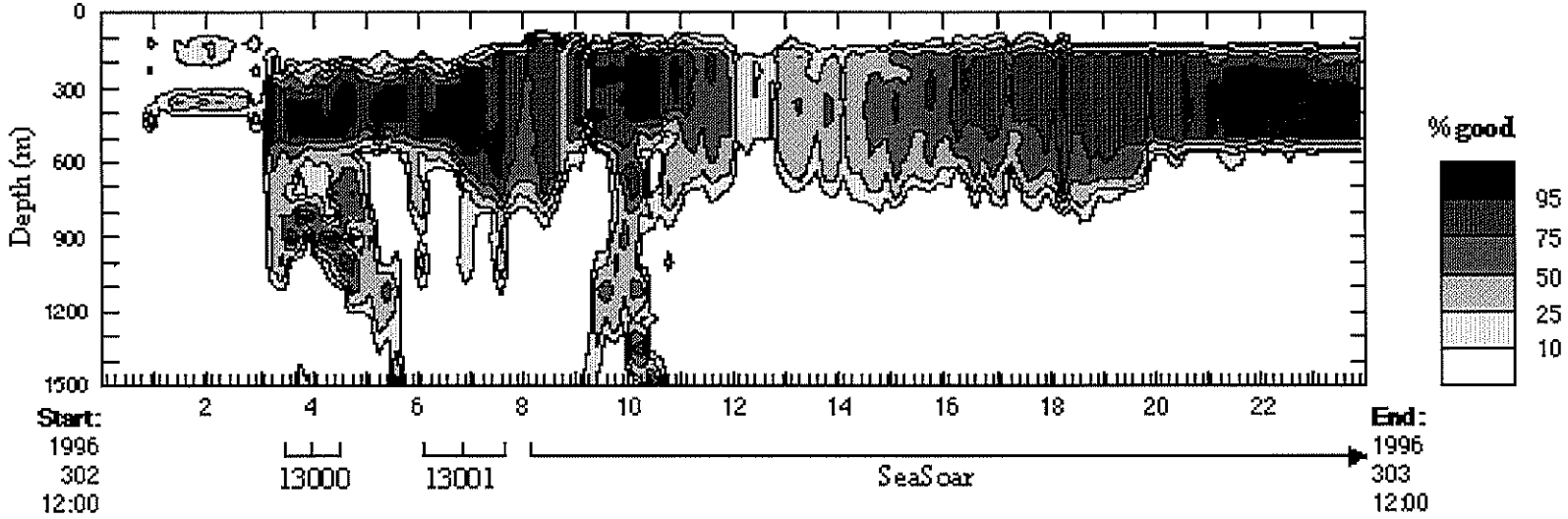

Figure 5.3.1: %good as a function of depth (m) and time (hours). The time axis covers 24 hours; start time (Year - Day - Hours:Minutes [UCT]) and end time (similarly) are shown. Cruise events (CTD stations [5-digit numbers] and SeaSoar tows) are shown on the time line above. The bottom is visible at station 13000 (depth 678 m).

Segment 5 Day 3

Figure 5.3.2: Significant wave height Hs (solid, left scale) and wind speed (grey, right scale) vs. time.

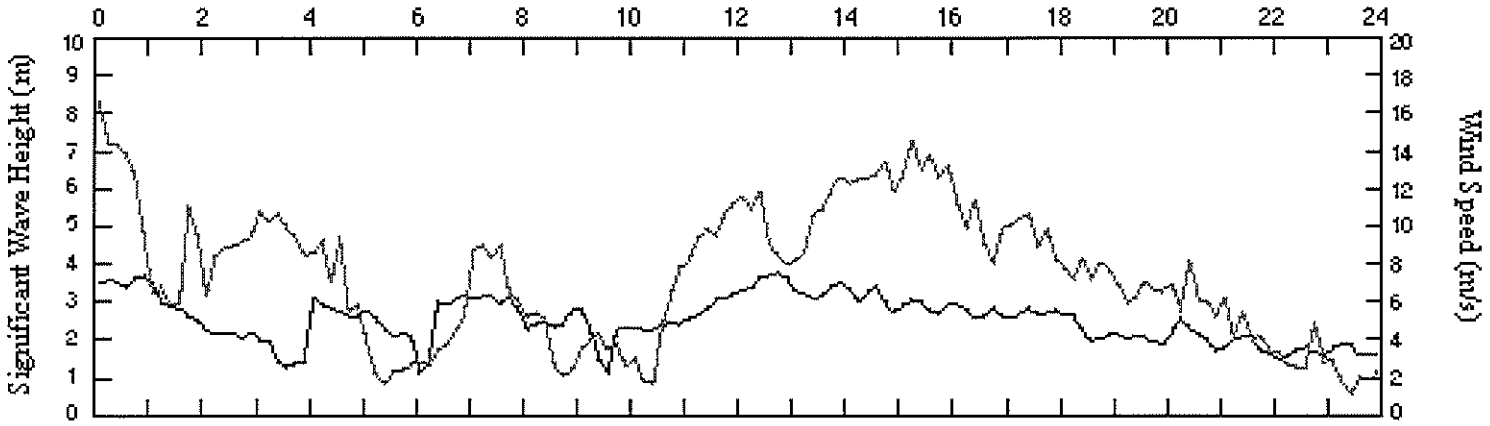

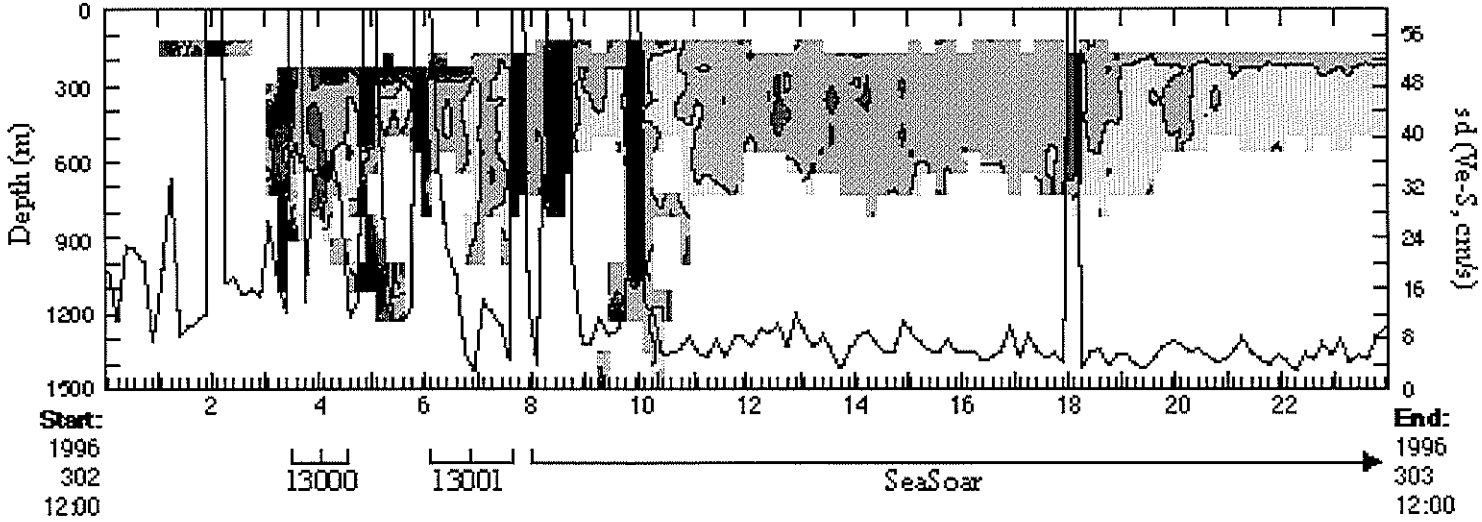

Figure 5.3.3: Standard deviation of east component of water velocity measured by ACCP [sd(Ve-A), contours], and standard deviation of east component of ship velocity over ground measured by differential GPS [sd(Ve-S), solid line, right scale]. Time axis as before.

Segment 5 Day 3

Figure 5.3.4: As above, for standard deviation of north velocity components: sd(Vn-A) and sd(Vn-S).

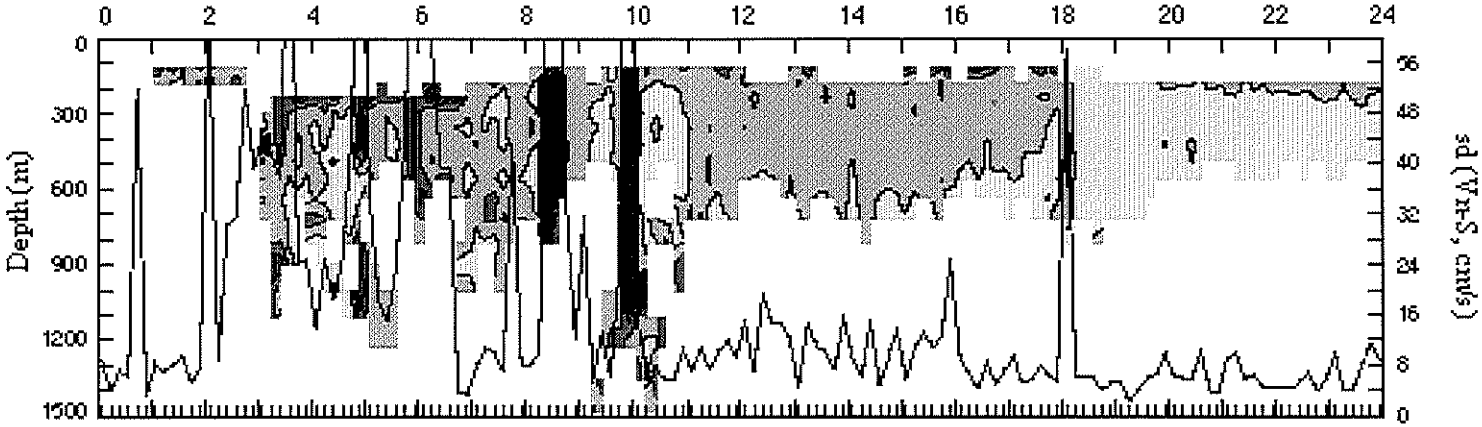

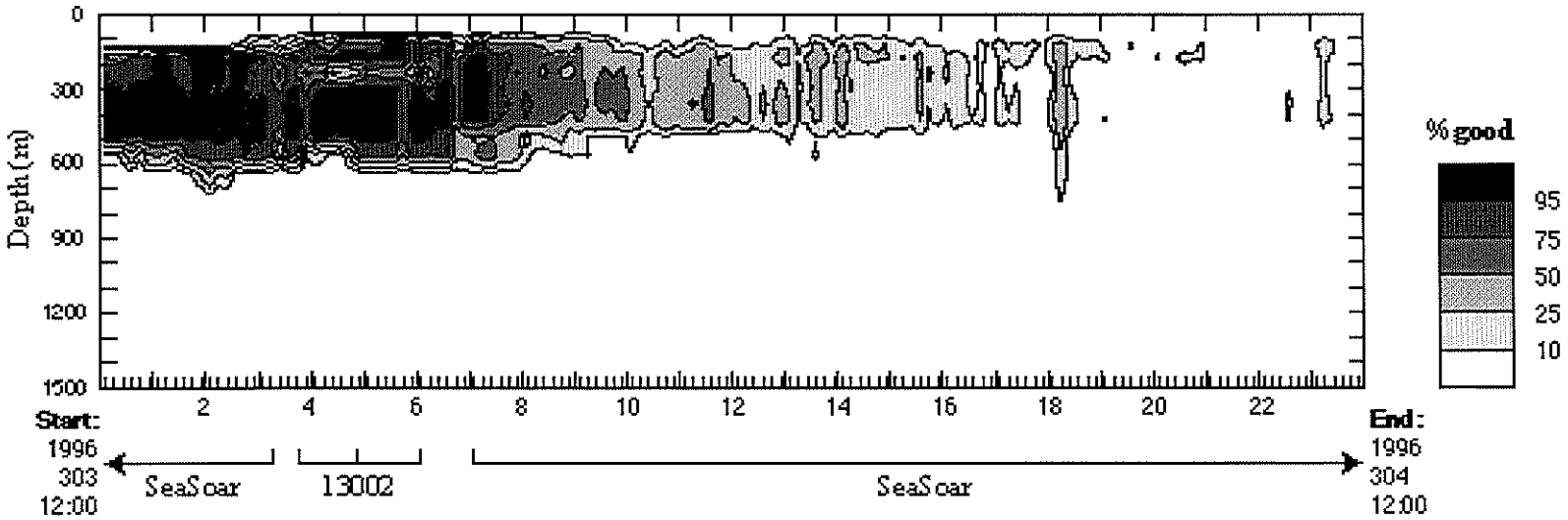

Figure 5.4.1: %good as a function of depth (m) and time (hours). The time axis covers 24 hours; start time (Year - Day - Hours:Minutes [UCT]) and end time (similarly) are shown. Cruise events (CTD stations [5-digit numbers] and SeaSoar tows) are shown on the time line above.

Segment 5 Day 4

Figure 5.4.2: Significant wave height Hs (solid, left scale) and wind speed (grey, right scale) vs. time.

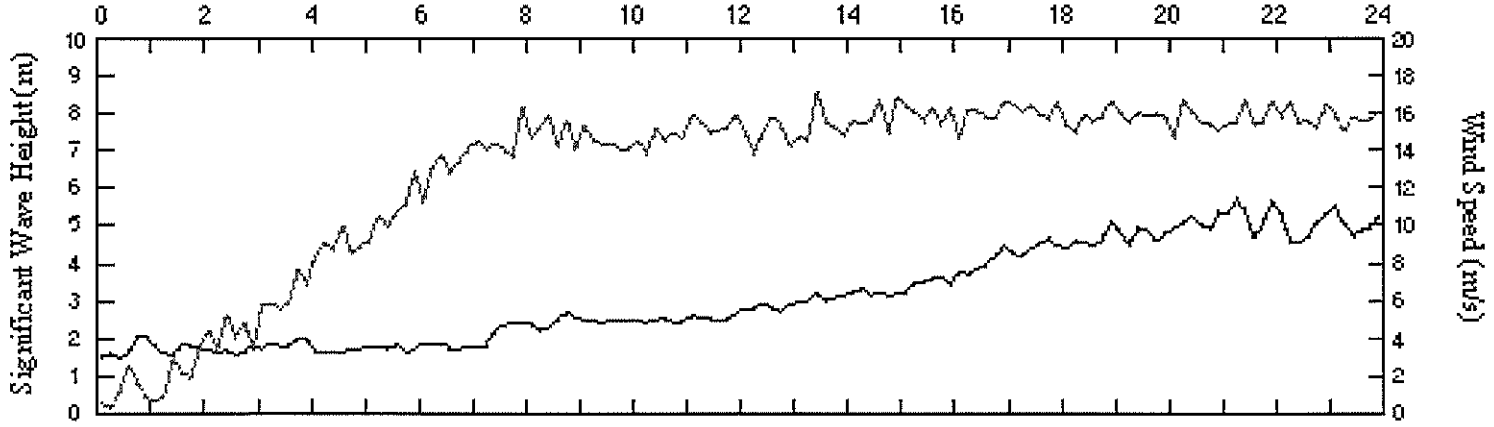

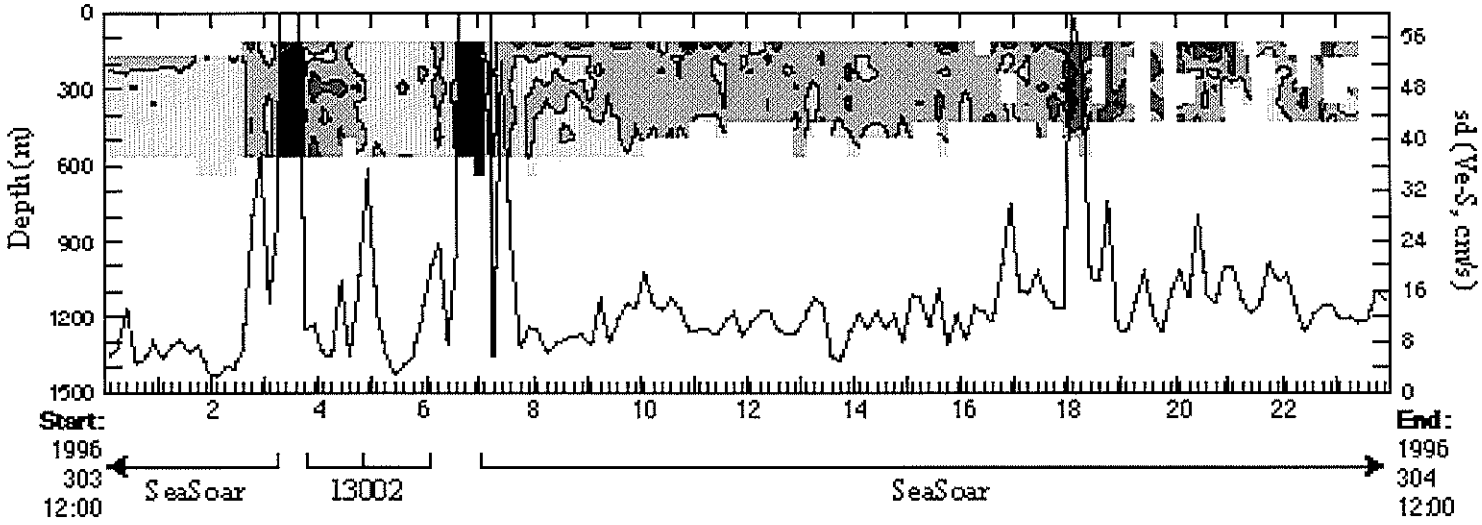

Figure 5.4.3: Standard deviation of east component of water velocity measured by ACCP [sd(Ve-A), contours], and standard deviation of east component of ship velocity over ground measured by differential GPS [sd(Ve-S), solid line, right scale]. Time axis as before.

Segment 5 Day 4

Figure 5.4.4: As above, for standard deviation of north velocity components: sd(Vn-A) and sd(Vn-S).

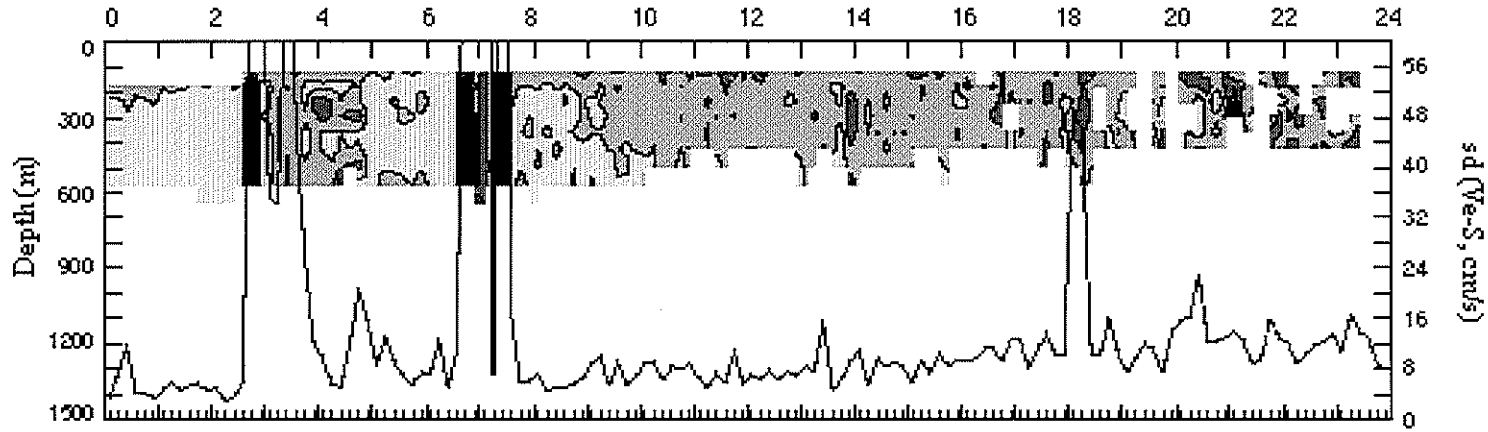

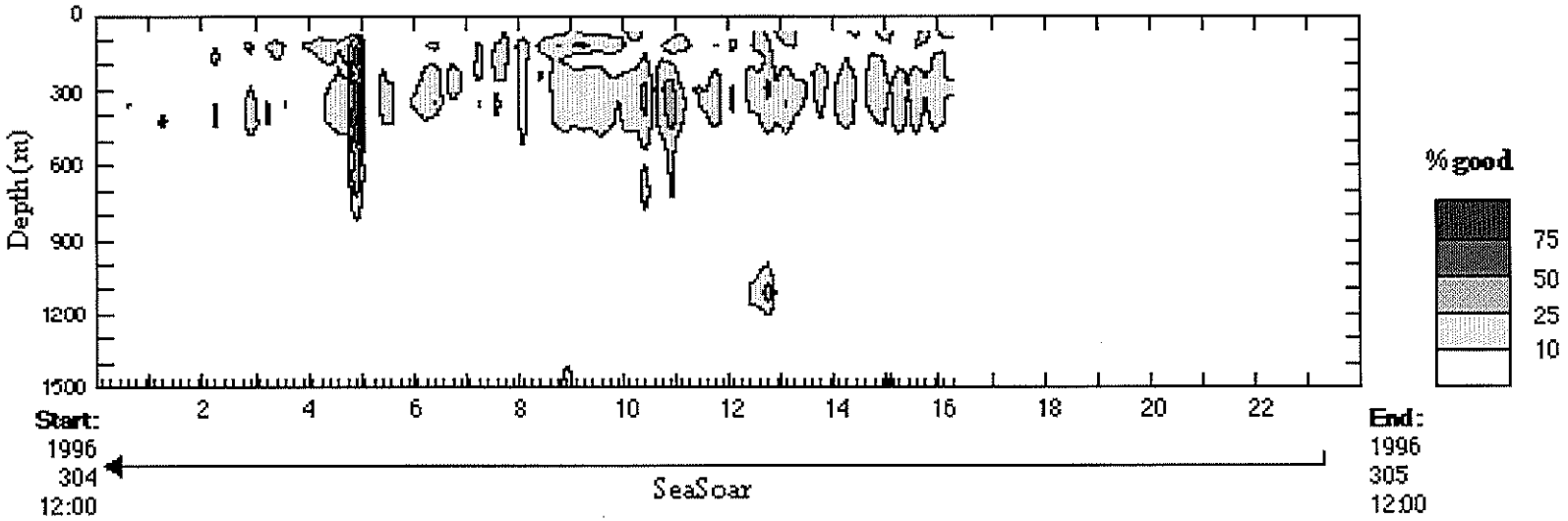

Figure 5.5.1: %good as a function of depth (m) and time (hours). The time axis covers 24 hours; start time (Year - Day - Hours:Minutes [UCT]) and end time (similarly) are shown. Cruise events (CTD stations [5-digit numbers] and SeaSoar tows) are shown on the time line above.

Segment 5 Day 5

Figure 5.5.2: Significant wave height Hs (solid, left scale) and wind speed (grey, right scale) vs. time.

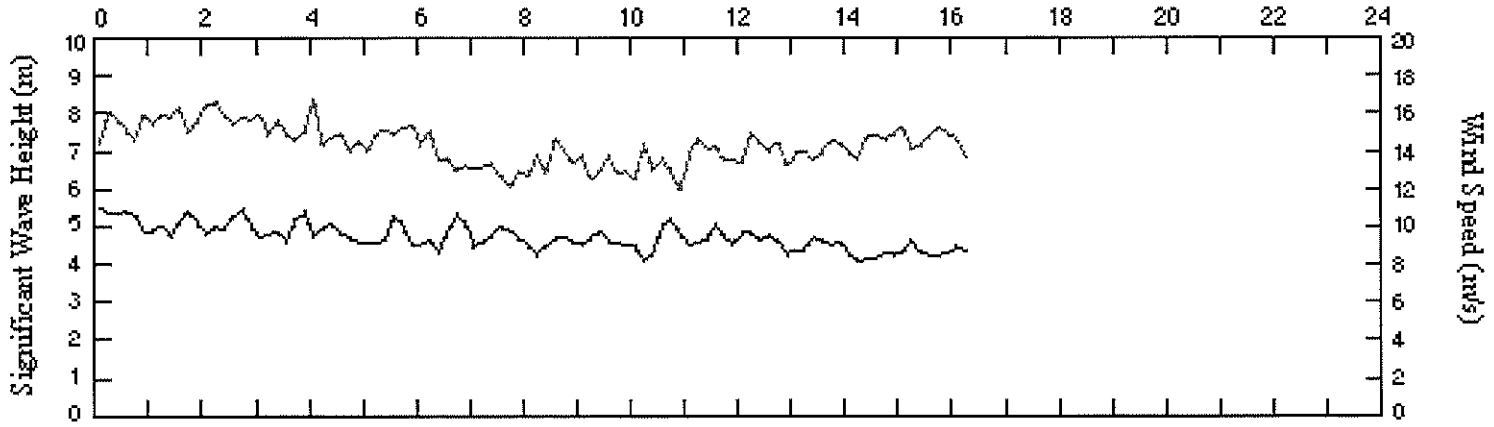

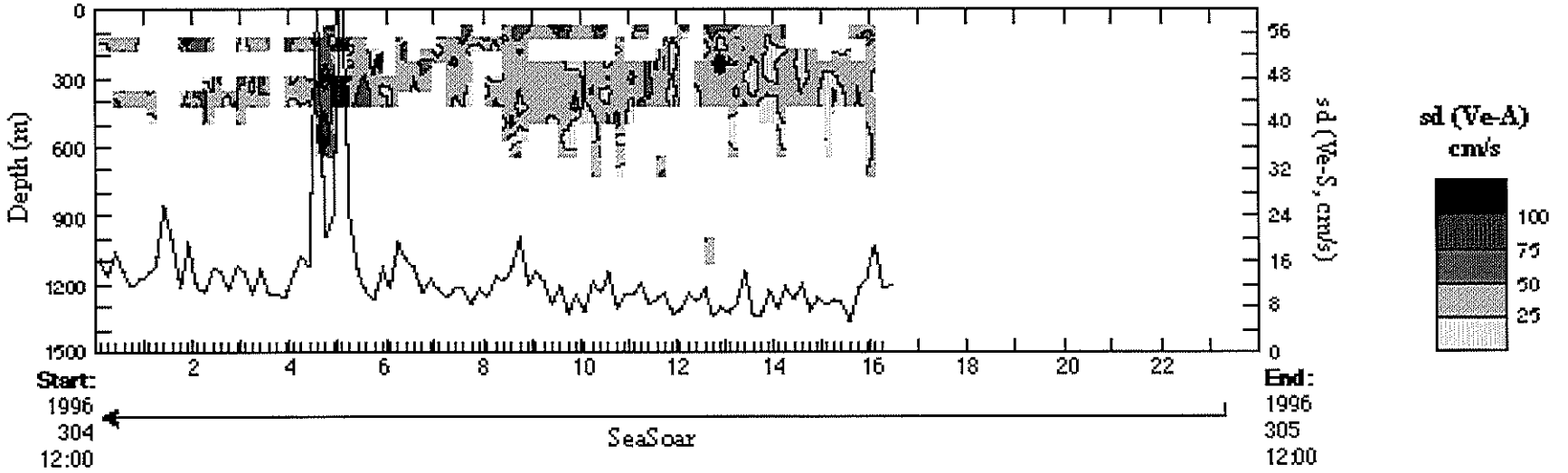

Figure 5.5.3: Standard deviation of east component of water velocity measured by ACCP [sd(Ve-A), contours], and standard deviation of east component of ship velocity over ground measured by differential GPS [sd(Ve-S), solid line, right scale]. Time axis as before.

Segment 5 Day 5

Figure 5.5.4: As above, for standard deviation of north velocity components: sd(Vn-A) and sd(Vn-S).

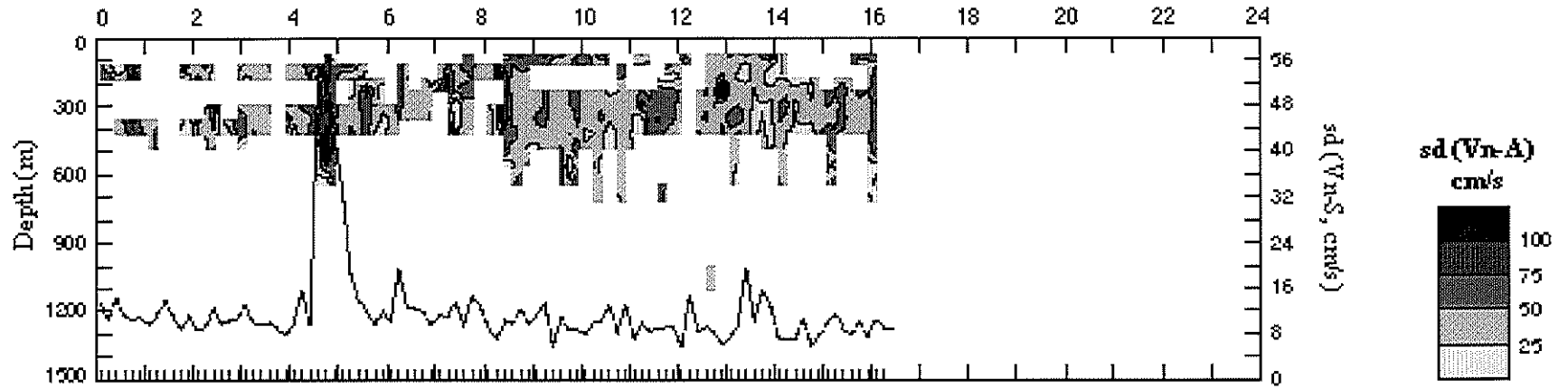

Fig. 6.1.1: %good

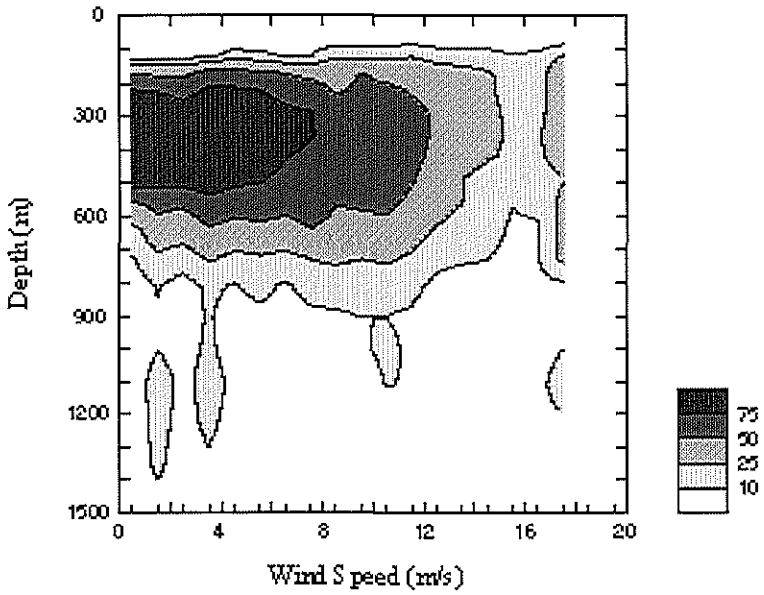

Fig. 6.1.2: sd (%good)

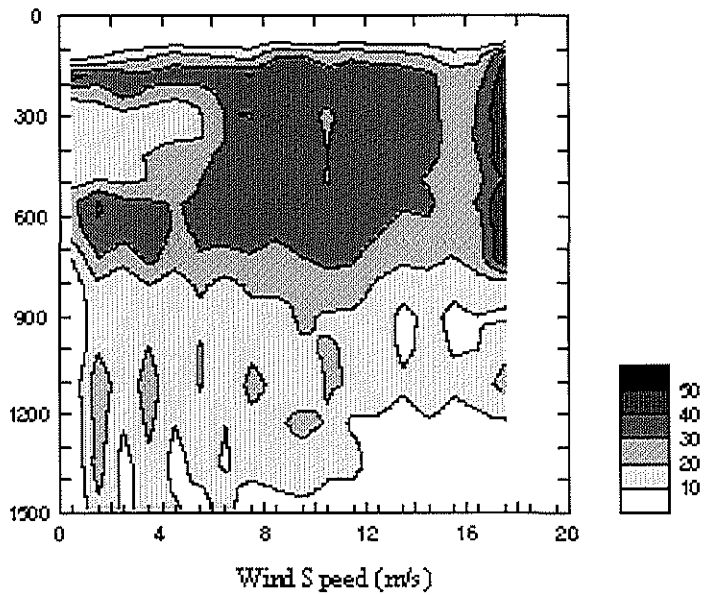

Fig. 6.1.3: Histogram of wind speed occurrences

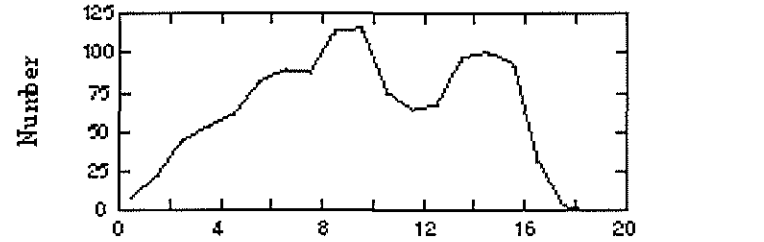

Fig. 6.1.4: Standard error of wind speed per bin

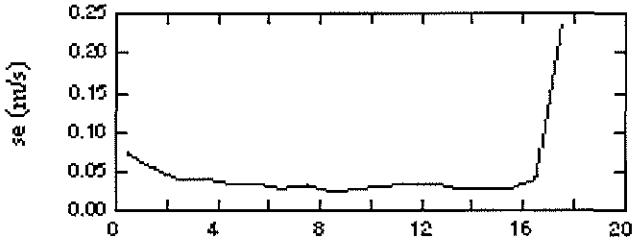

Figure 6.1: Analysis of %good as a function of wind speed and depth for all data in fig. 6.1.1. Wind speed is in 1 m/s bins. Standard deviation of %good per bin [sd(%good)] in fig. 6.1.2. Total number of occurrences of wind speeds per bin as histogram in fig. 6.1.3. Standard error of wind speed per bin (se) in fig. 6.1.4.

Fig. 6.2.1: %good

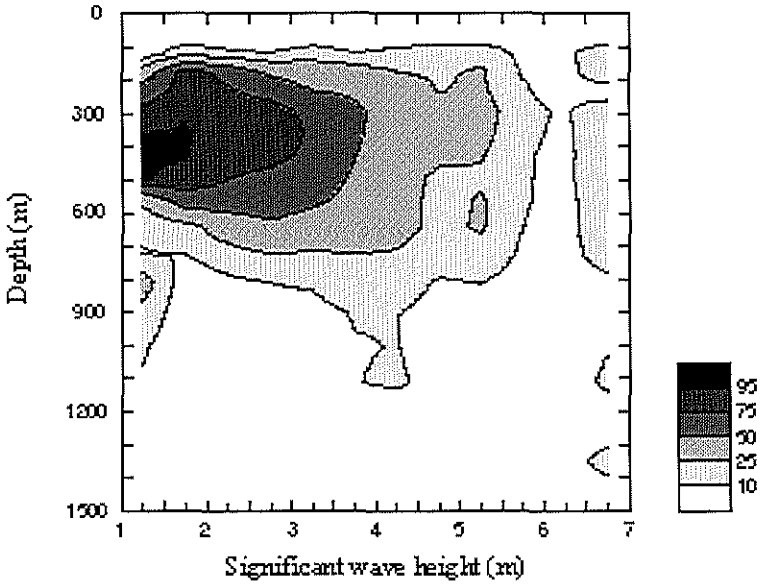

Fig. 6.2.2: sd (%good)

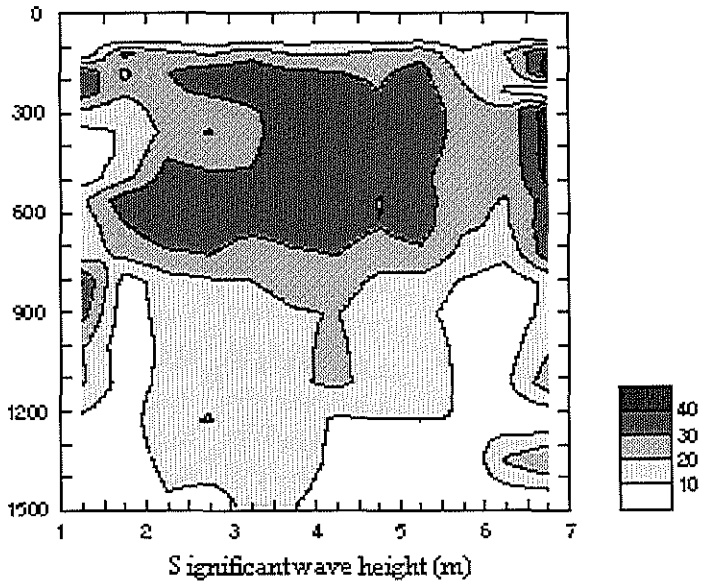

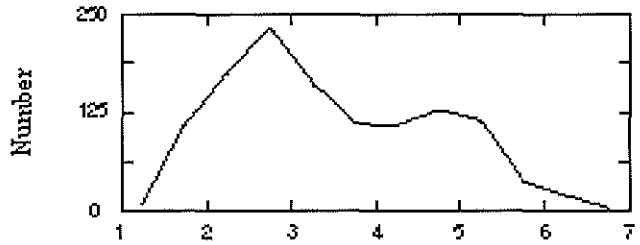

Fig. 6.2.3: Histogram of Hs occurrences

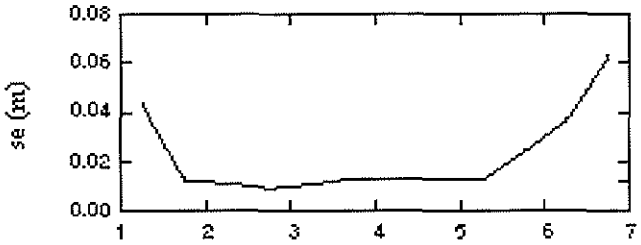

Fig. 6.2.4: Standard error of Hs per bin

Figure 6.2: Analysis of %good as a function of significant wave height (Hs) and depth for all data in fig. 6.2.1. Hs is in 0.5 m bins. Standard deviation of %good per bin [sd(%good)] in fig. 6.2.2. Total number of occurrences of Hs per bin as histogram in fig. 6.2.3. Standard error of Hs per bin (se) in fig. 6.2.4.

Fig. 6.3.1: %good

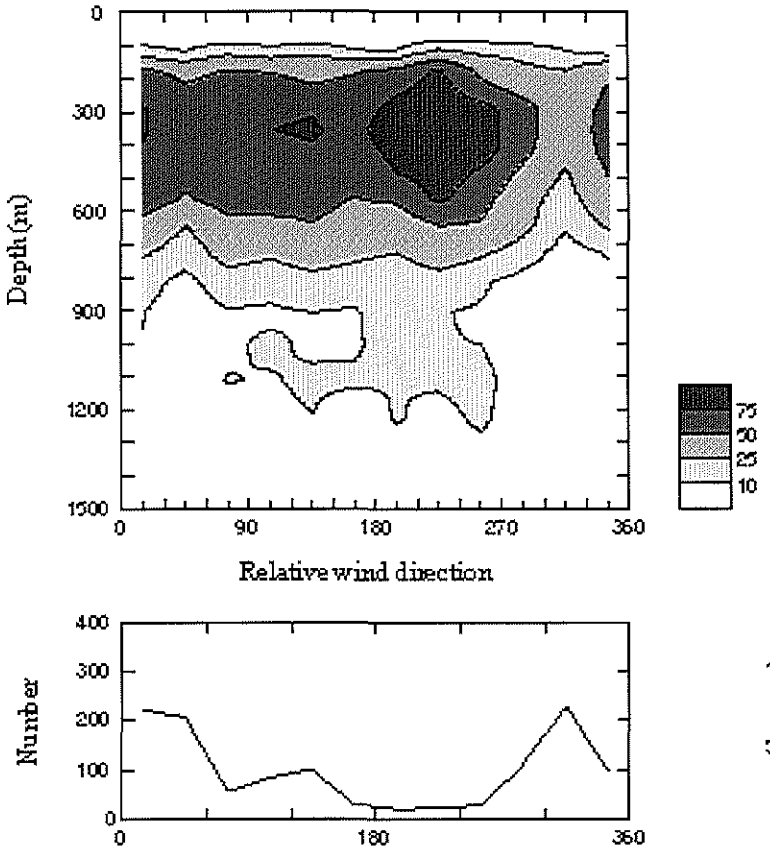

Fig. 6.3.2: sd(%good)

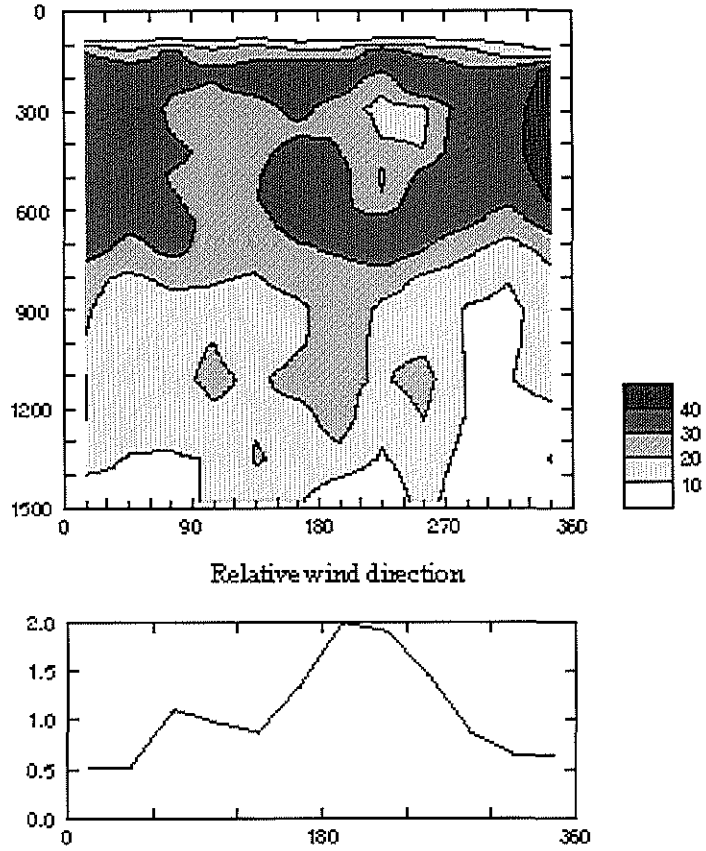

Fig. 6.3.3: Histogram of relative wind direction occurrences

Fig. 6.3.4: Standard error of relative wind direction per bin

Figure 6.3: Analysis of %good as a function of relative wind direction and depth for all data in fig. 6.3.1. Relative wind direction is in 30° bins. Standard deviation of %good per bin [sd(%good)] in fig. 6.3.2. Total number of occurences of relative wind direction per bin as histogram in fig. 6.3.3. Standard error of relative wind direction per bin (se) in fig. 6.3.4.

Fig. 6.4.1: %good

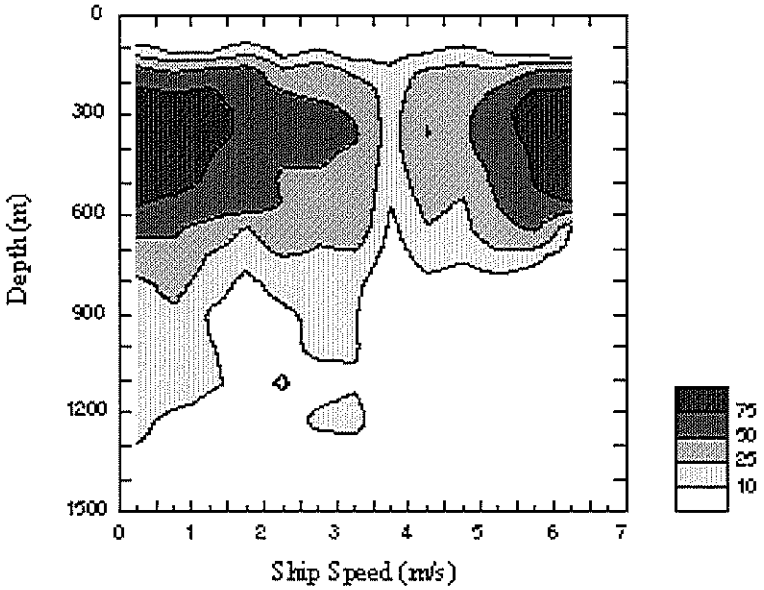

Fig. 6.4.2: sd(%good)

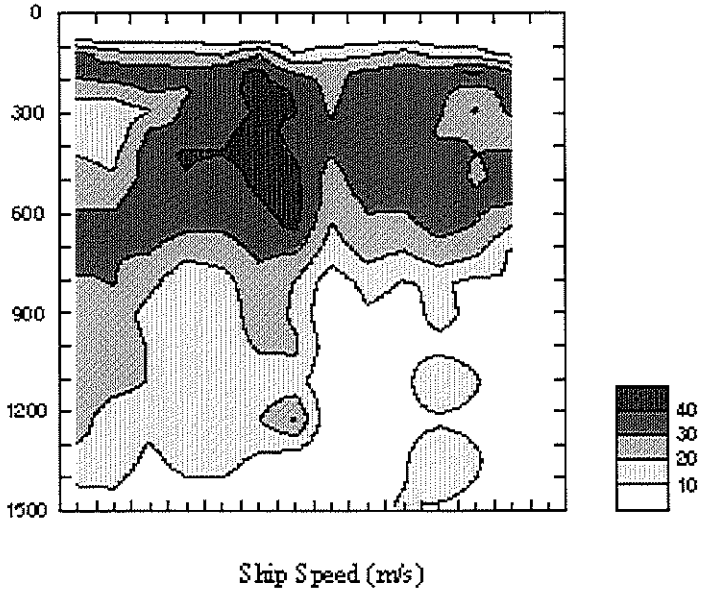

Fig. 6.4.3: Histogram of ship speed occurrences

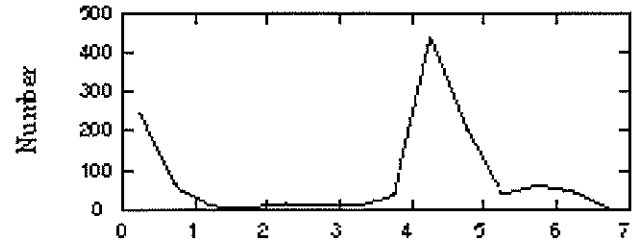

Fig. 6.4.4: Standard error of ship speed per bin

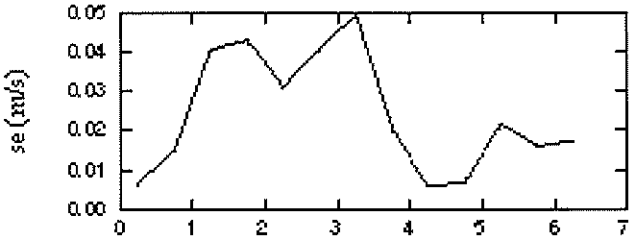

Figure 6.4: Analysis of %good as a function of ship speed and depth for all data in fig. 6.4.1. Ship speed is in 0.5 m/s bins. Standard deviation of %good per bin [sd(%good)] in fig. 6.4.2. Total number of occurrences of ship speeds per bin as histogram in fig. 6.4.3. Standard error of ship speed per bin (se) in fig. 6.4.4.

Fig. 7.1.1: Station 12942 east velocity components

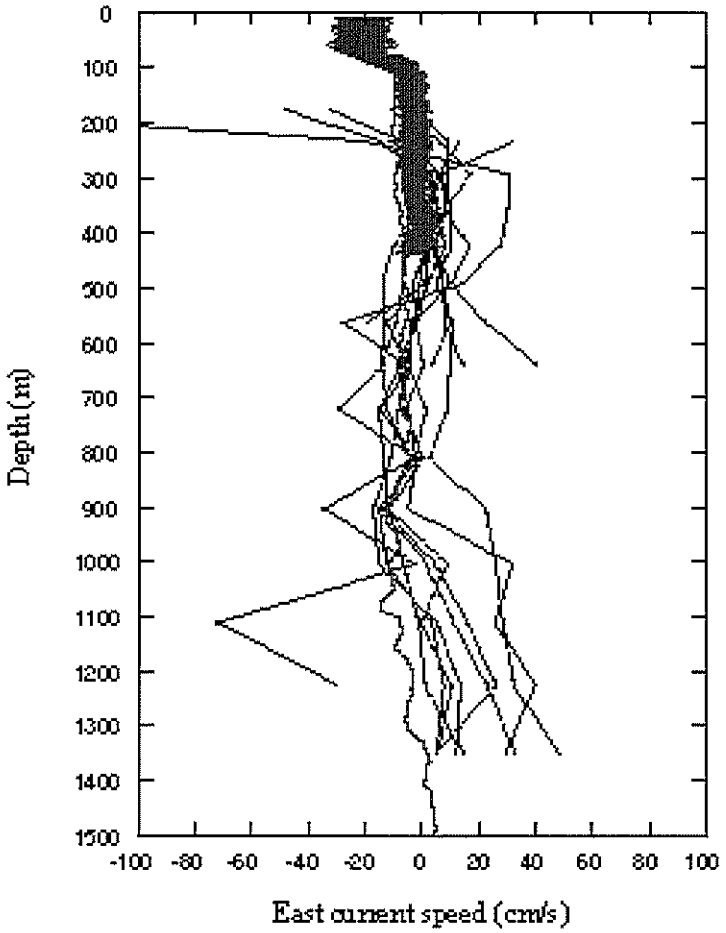

Fig. 7.1.2: Station 12942 north velocity components

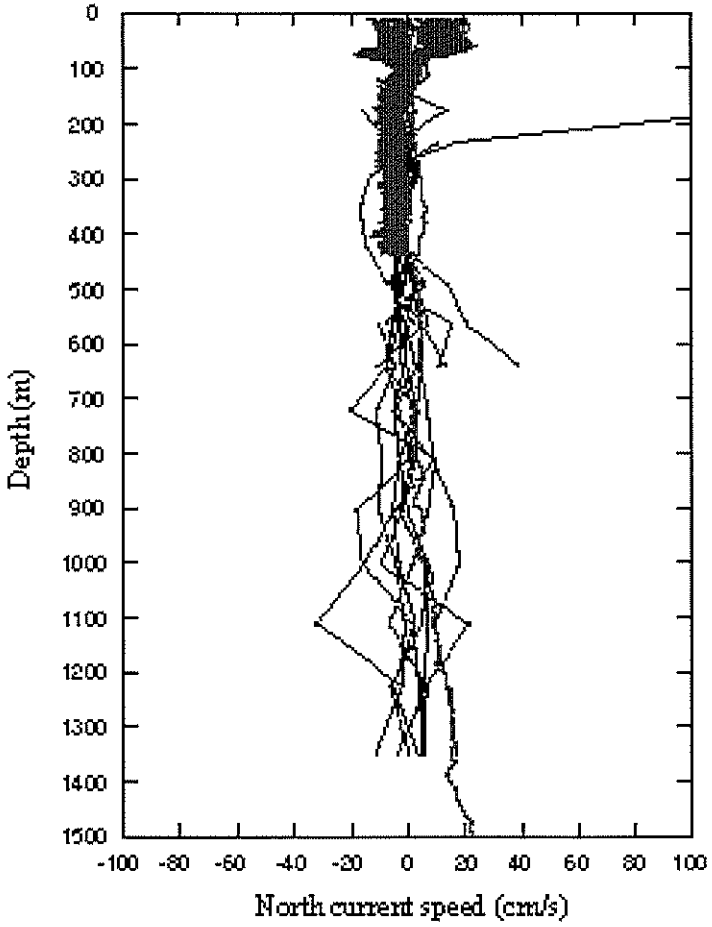

Figure 7.1: Water velocity components (east, fig. 7.1.1 and north, fig. 7.1.2, cm/s) measured during station 12942 by VM-ADCP (green), L-ADCP (red) and ACCP (black).

Fig. 7.2.1: Station 12985 east velocity components

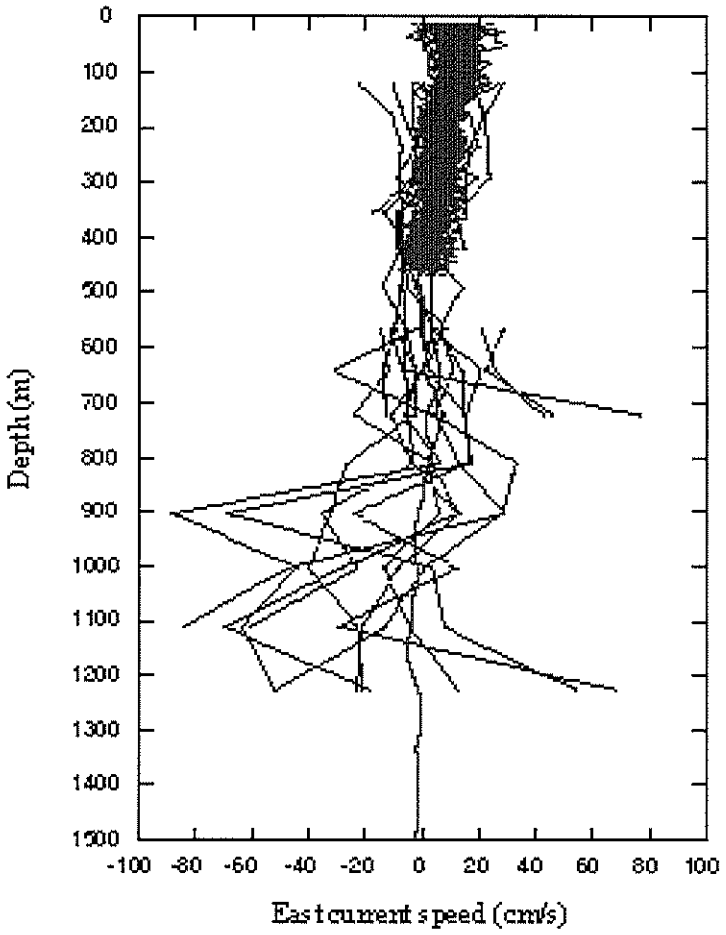

Fig. 7.2.2: Station 12985 north velocity components

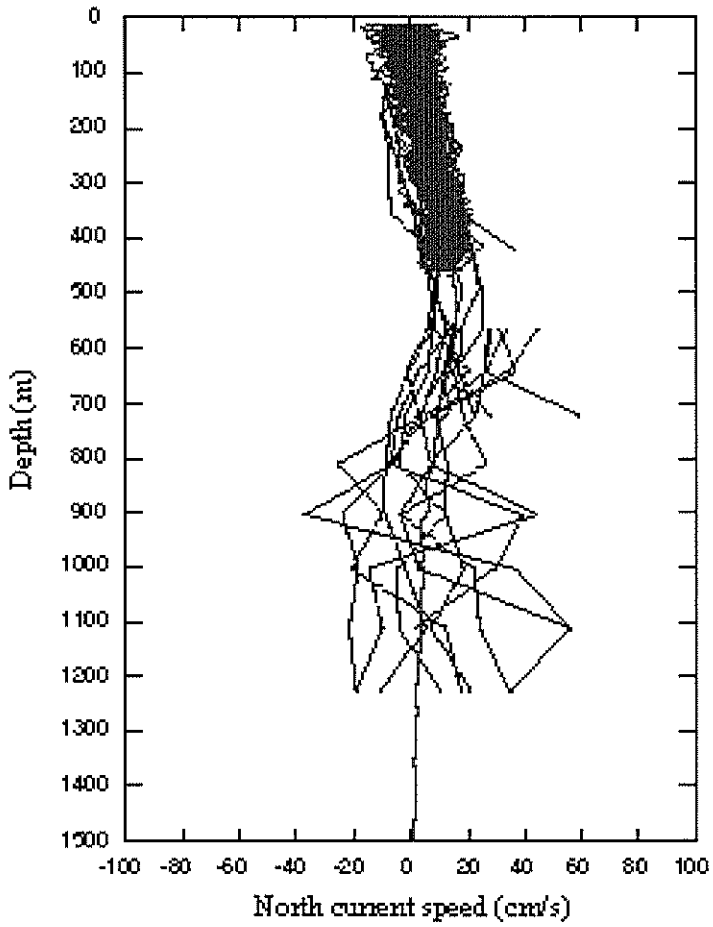

Figure 7.2: Water velocity components (east, fig. 7.2.1 and north, fig. 7.2.2, cm/s) measured during station 12985 by VM-ADCP (green), L-ADCP (red) and ACCP (black).

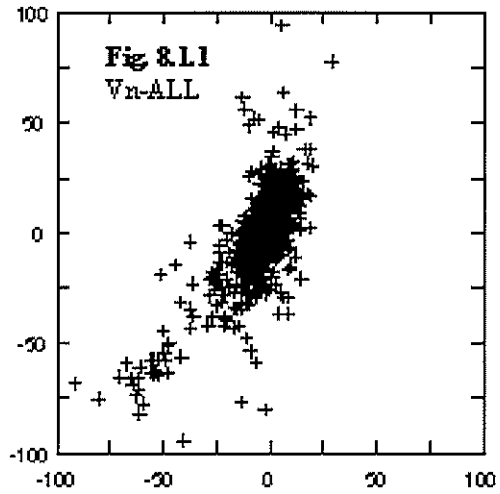

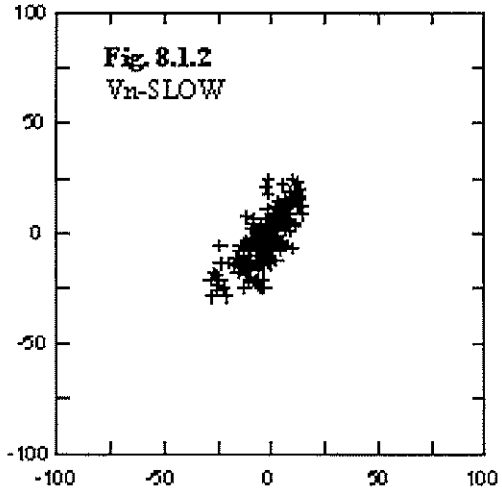

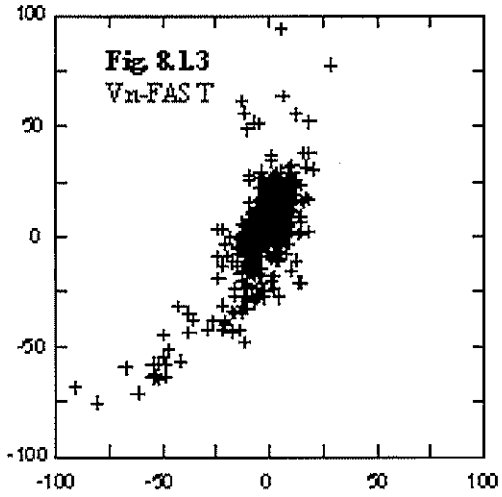

Figure 8.1: Figures on this page show comparisons between VM-ADCP data (X-axes) and ACCP data (Y-axes) for north velocity components (Vn, cm/s, above) and east velocity components (Ve, cm/s, below) at the 356 m depth ACCP bin and an equivalent vertical mean of VM-ADCP bins. See text for further explanation. All data are presented in figs. 8.1.1 and 8.1.4 (ALL); data are subselected for ship speed less than 1 knot in figs. 8.1.2 and 8.1.5 (SLOW), and greater than 8 knots in figs. 8.1.3 and 8.1.6 (FAST).

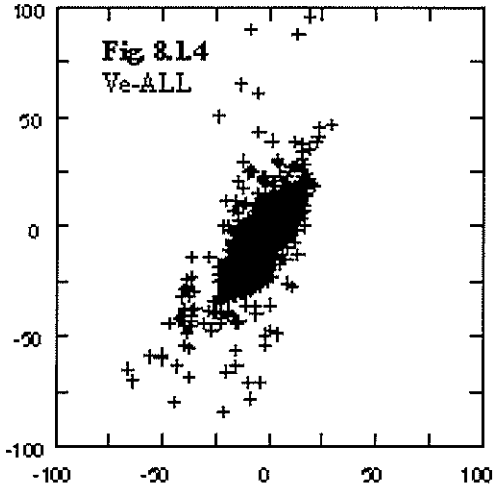

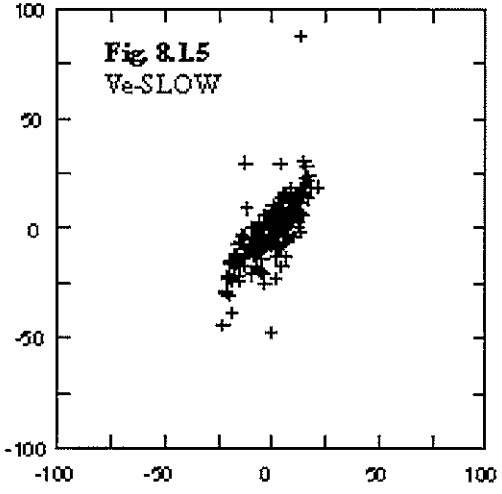

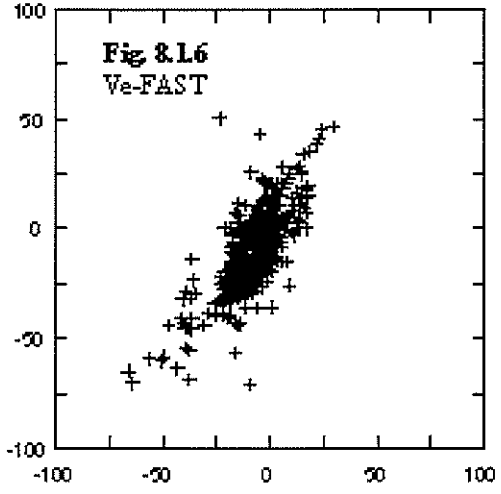

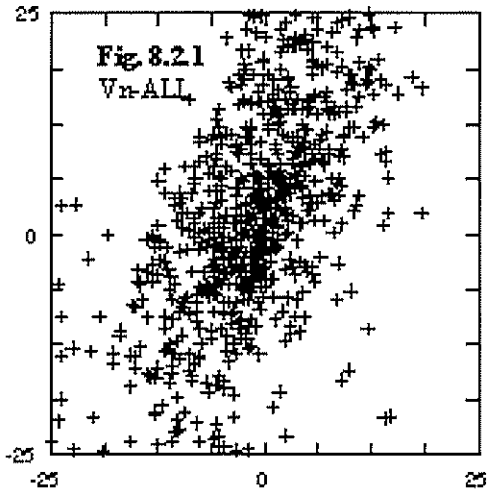

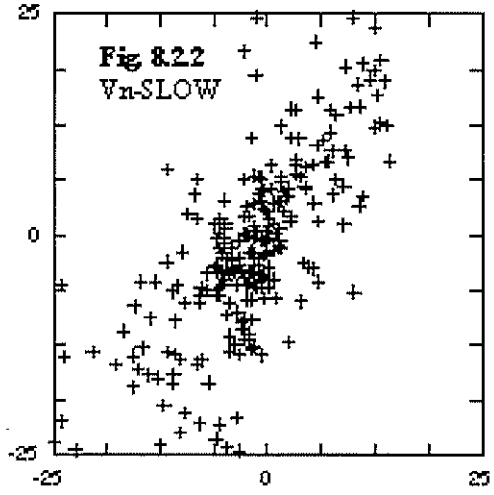

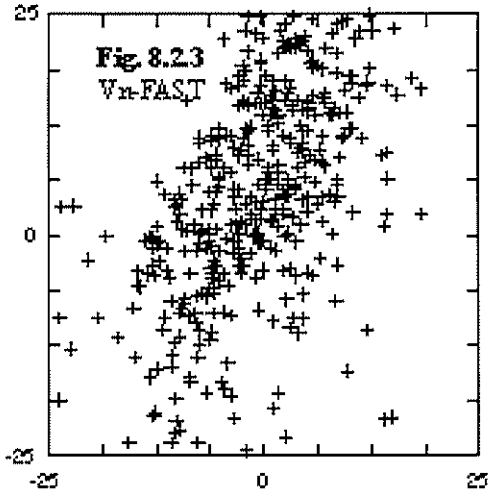

Figure 8.2: Figures on this page show comparisons between VM-ADCP data (X-axes) and ACCP data (Y-axes) for north velocity components (Vn, cm/s, above) and east velocity components (Ve, cm/s, below) at the 356 m depth ACCP bin and an equivalent vertical mean of VM-ADCP bins at an enhanced scale over fig. 8.1. See text for further explanation. All data within range are presented in figs. 8.2.1 and 8.2.4 (ALL); data are subselected for ship speed less than 1 knot in figs. 8.2.2 and 8.2.5 (SLOW), and greater than 8 knots in figs. 8.2.3 and 8.2.6 (FAST).

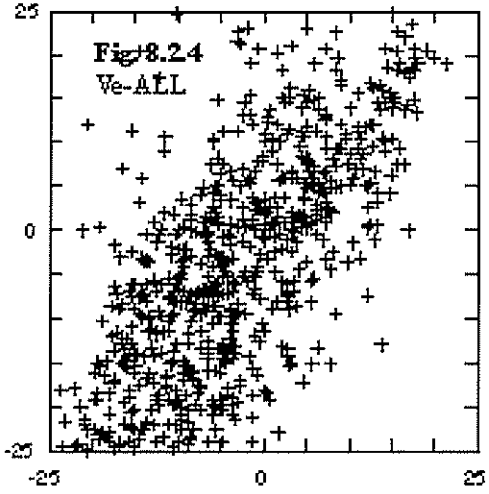

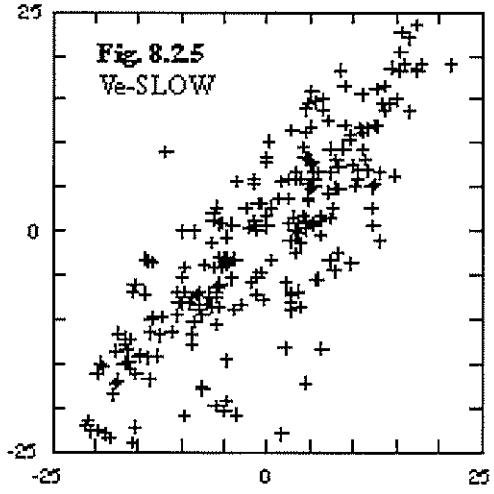

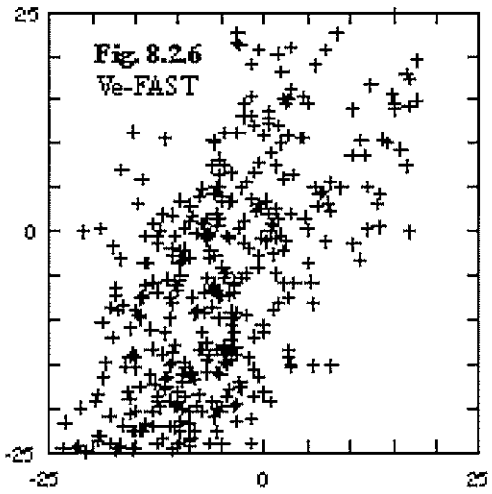

Figure 9.1: Comparison of east velocity components

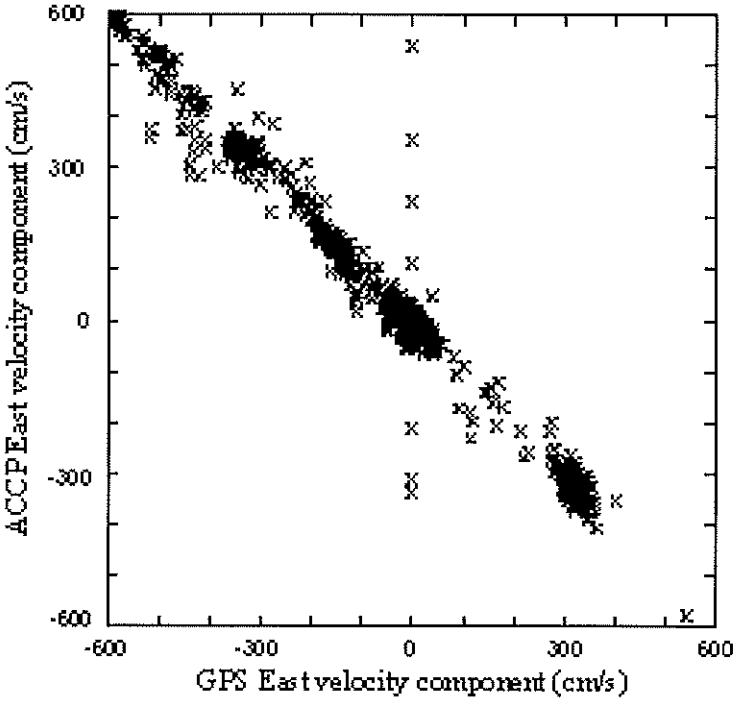

Figure 9.2: Comparison of north velocity components

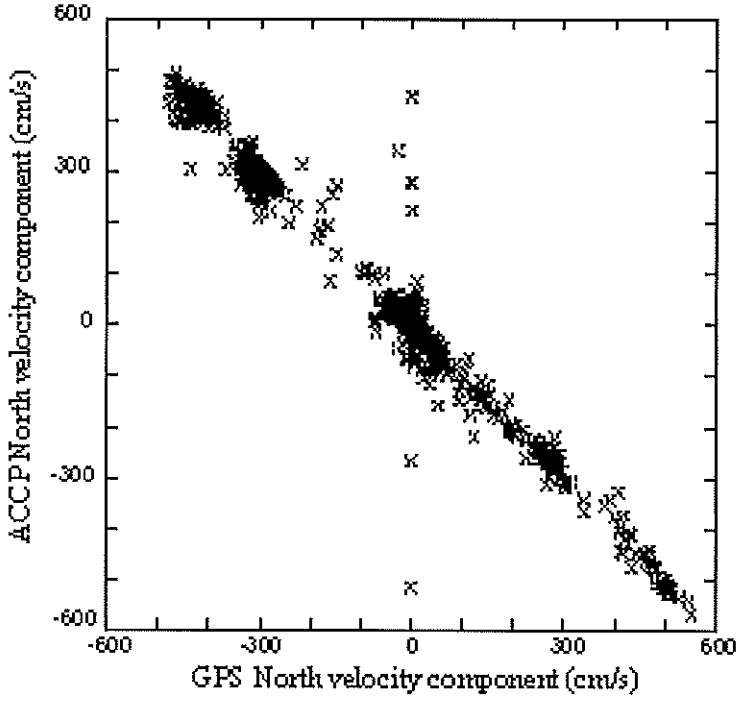

Figure 9: Comparison of north and east velocity components of ship velocity over the ground via differential GPS with water velocity past the ship from the ACCP.